MASTERS THESIS

Exploring Spaceborne Snowfall Retrieval Biases Using a Long Term Ground Based Profiling Radar in Barrow, AK

Author:
William HAHN

Supervisor:
Mark KULIE
Tristan L'ECUYER

*A thesis submitted in fulfillment of the requirements
for the degree of*

Master of Science

in the

Atmospheric and Oceanic Sciences

2017

Declaration of Authorship

I, William HAHN, declare that this thesis titled, "Exploring Spaceborne Snowfall Retrieval Biases Using a Long Term Ground Based Profiling Radar in Barrow, AK" and the work presented in it are my own. I confirm that:

William Hahn
Author   Signed: Date:

I hereby approve and recommend for acceptance this work in partial fulfillment of the requirements for the degree of Master of Science:

Mark Kulie
Committee Chair   Signed: Date:

Tristan L'Ecuyer
Faculty Member   Signed: Date:

Grant Petty
Faculty Member   Signed: Date:

University of Wisconsin Madison

Abstract

Atmospheric and Oceanic Sciences

Master of Science

Exploring Spaceborne Snowfall Retrieval Biases Using a Long Term Ground Based Profiling Radar in Barrow, AK

by William HAHN

A seven-year dataset using observations from a ground based millimeter wavelength cloud radar (MMCR) was created to enable unique high latitude snowfall research. The MMCR is located in Barrow, AK at the Atmospheric Radiation Measurement (ARM) North Slope Alaska (NSA) Climate Research Facility. Beyond radar measurements, this site features a surface meteorological instrument (Surface MET), which when combined with the radar, provides robust information about the weather in this region. Barrow, AK frequently receives shallow snowfall events where cloud top heights are below 1-2 km. These shallow snowfall events pose many measurements issues for spaceborne radar platforms, because due to ground clutter and other issues at the surface, measurements below this level are unreliable creating a measurement blindzone in the lowest 1 km above ground level. Conducting this study at a site with frequent light (low reflectivity) and shallow snowfall events offers an opportunity to observe what current and potential spaceborne radar platforms may miss blindzone when snowfall events are in the blindzone and what snowfall regimes are dominant in this region. To ensure a thorough examination at this site, several environmental parameters including sea ice coverage were analyzed to identify snowfall regime's dependencies to these various factors, which overall resulted in expected trends. MMCR near surface bins were not well correlated with MMCR data bins

near 1 km for shallow snowfall events, thus reflecting possible systematic issues for spaceborne radars that utilize near surface bins at 1 km for surface snowfall retrievals. Snowfall events can vary on a daily and yearly scale, but the predominate feature is shallow and light snowfall events with about 50% of total snowfall occurrences and 6% of total accumulation occurrences falling below 1 km in cloud level. For snowfall events below 2 km in cloud top height, there was just over a 6 dBZ negative bias measured from 1 km to the surface, meaning there would likely be an underestimation of reflectivity at the surface. When utilizing CloudSat's threshold of -15 dBZ for snow-probable cases, it is shown that -15 dBZ misses over half of the total snowfall occurrences, but accounts for almost all of the snowfall accumulation occurrences. With emphasis on the 1 km blindzone level, just over 13% of total snowfall occurrences and 8% of total accumulation occurrences, which would be deemed snow probable via CloudSat, would likely be missed. If spaceborne radar platforms were to decrease the blindzone to 500 m, these values, along the negative radar bias, could be decreased by over half.

Acknowledgements

Mark Kulie: For helping me through each step of this project from basic programming help to the writing of this thesis, I appreciate any and all help you have given me during this project

Tristan L'Ecuyer: For always offering fresh ideas and ways to further advance the project and contributing the necessary extra inspection on my work

Undergraduate and Graduate colleagues for their support inside and outside of the classroom

Colleagues and Faculty of the Atmospheric and Oceanic Sciences Department and Space Sciences and Engineering Center

My family for always supporting me throughout my life with everything

Dedicated to my parents Ed and Teri Hahn and my Grandparents, Grandma Volkman and Grandpa and Grandma Hahn

Dad: Thanks for all of your advice and continuing to push me to become successful

Mom: Thank you for your never ending support and willingness to help

Grandma Volkman: Thanks for taking me in whenever and always being welcoming and accommodating

Grandpa and Grandma Hahn: Thank you for your encouragement in everything that I do

Contents

List of Figures

List of Abbreviations

ARM	**A**tmospheric **R**adation **M**easurment
CFAD	**C**ontoured **F**requency by **A**ltitude **D**iagram
CPR	**C**loud **P**rofiling **R**adar (aboard CloudSat)
DPR	**D**ual-Frequency **P**recipitation **R**adar
GPM	**G**lobal **P**recipitation **M**easurment
MMCR	**M**illi**m**eter **C**loud **C**adar
NEXRAD	**NEX**t Generation **RAD**ar
NMQ	**N**ational **M**osaic and Multi-Sensor **Q**PE
NSA	**N**orth **S**lope **A**laska
NSIDC	**N**ational **S**now and **I**ce **D**ata **C**enter
PWD	**P**resent **W**eather **D**etector
PWS	**P**resent **W**eather **S**ystem
TRMM	**G**lobal **P**recipitation **M**easurment
WSR-88D	**W**eather **S**urveillance **R**adar 19**88** **D**oppler

Chapter 1

Introduction

High latitude precipitation is important and arguably an understudied area of study using observational datasets. Much of the precipitation in the high latitudes is snowfall, which has an integral role in the Earth system. Snowfall is mostly limited to high latitudes and mountainous regions (Kulie et al. 2016). This makes studying snowfall increasingly interesting, since these regions are more sensitive to a warming climate, which is a heavily studied topic in Barrow, AK (Hinzman et al.). There are two main types of snowfall based on cloud regimes. Snowfall events are usually described as deep or shallow based on their respective vertical cloud structures. Both are relatively unique and pose interesting research questions for study as to the impacts each regime can have when they occur. To study and measure these types of snowfall, multiple methods can be employed, but the two most common include ground-based observations and observations via satellite.

In order to measure snowfall on a ground level, RAdio Detection and Ranging (RADAR) are the best tools for measurement. An example of a precipitation detecting radar is the millimeter cloud radar (MMCR) from the Atmospheric Radiation Measurement Climate Research Facility at the North Slope Alaska site in Barrow, AK. The MMCR in Barrow, allows for the ability to measure multiple facets of snowfall from a ground-based radar and is the radar from which this research utilizes data from. There is a small network of MMCR's and radars much like it across the world allowing for some spatial coverage of snowfall measurements using ground-based radar observations. Using ground-based radars to measure Earth's snowfall is a difficult task due to the overall lack of spatial coverage in remote regions in high latitudes. The current

most optimal way to measure snowfall on a global scale is through spaceborne radar platforms. There has been a global effort to incorporate satellite observations into overall snowfall retrievals by using spaceborne radar platforms. These platforms include the satellites CloudSat and the Global Precipitation Measurement Mission (GPM). CloudSat uses a Cloud Profiling Radar (CPR), which is great for detecting and measuring snowfall accumulation. Meanwhile, GPM utilizes a Dual Profiling Radar (DPR) to measure precipitation. Both of these satellites have improved overall global retrievals of precipitation.

While CloudSat and GPM are excellent tools to utilize in order to make global precipitation observations, neither satellite is perfect and improvements can be made. GPM has a limited orbital extent and a high minimum detectable reflectivity, making it not optimal for snowfall retrievals. CloudSat has much more global coverage and much lower minimum reflectivity, but is limited by a 'blindzone' where due to various factors, observations below one kilometer above ground level are very unreliable. Ground-clutter contamination is the main reason for the blindzone and has contributed to up 1 dB of underestimation for reflectivity and the amount of precipitation being underestimated by about 10% (Maahn et al.). Ground-based radars can make up for this deficit with more accurate observations in CloudSat's blindzone, but spatial coverage and remoteness of the radars are two main limiting factors. Reliability is very good for ground-based radars, however, they just don't have the spatial capabilities for measurements to made on a global scale like CloudSat can, thus making spaceborne radar platforms a necessary tool to make the best possible global scale precipitation observations. Overall, the NSA dataset serves as a great CloudSat evaluation tool so we better understand pan-Arctic snowfall as well as understand the implications of the areas of improvement for CloudSat and other current and near future spaceborne radar platforms.

Chapter 2

Background

2.1 CloudSat & GPM

NASA's CloudSat satellite, launched in 2006, houses the first spaceborne W-band radar (94 GHz) (Stephens et al. 2002; Tanelli et al. 2008). This nadir-pointing cloud profiling radar (CPR) is used to study cloud occurrence, cloud macrophysical and microphysical properties, and cloud radiative effects. While not its primary mission of studying clouds, CPR observations offer extremely valuable precipitation estimates around the world, largely due to CloudSat's orbital extent of |82°| latitude (Kulie and Bennartz 2009; Kulie et al. 2016). This latitudinal range results in near global spatial coverage. Another feature of the CPR is it's minimum detectable reflectivity of approximately -30 dBZ, which allows it to observe most light precipitation and is very beneficial to measuring regions that frequently experience light precipitation events (Liu 2008). These two features allow CloudSat to have an advantage in measuring snowfall, especially at higher latitudes when compared to Global Precipitation Measurement (GPM), which is the current foremost global precipitation measurement satellite system that carries a dual frequency precipitation radar. GPM is limited to a |65°| orbital extent and a 12 dBZ radar minimum detectable reflectivity, which makes CloudSat a much more relevant comparison tool for this study due to the fact that Barrow, AK has a higher latitude than 65°N and is one key reason why CloudSat is currently the best way to observe snowfall on a global scale (Hou et al. 2014).

CloudSat is one part of NASA's afternoon constellation, the "A-Train," which allows its observations to be coupled with other "A-Train" satellites that have

unique observational capabilities to provide more detailed observations for various parameters. CloudSat has two levels of data products as well as an auxiliary data product level. One main product of interest includes the 2B-CLDCLASS product, which is able to classify different cloud types and is further discussed in more detail in the following Shallow Snowfall section. The other product of interest is the 2C-SNOW-PROFILE product, which provides estimates of vertical profiles of snowfall rate along with snow size distribution parameters and snow water content (Wood et al. 2013).

CloudSat's snowfall estimate data has been compared to many ground-based snowfall measuring systems in the past to evaluate results for either tool. Hiley et al. (2011) used ground-based snow gauges in Canada to test the accuracy of CloudSat's snowfall retrievals. The results were mixed as lower latitude samplings generally saw underestimation, while higher latitude samplings were much more accurate due to a higher likelihood of the precipitation being frozen and greater temporal coverage (Hiley, Kulie, and Bennartz 2011). Liu (2008) observed that, overall, retrievals were more accurate when the precipitation was much more likely to be frozen based on comparisons in Antarctica, where comparison results were very similar with precipitation consisting only of snowfall (Liu 2008; Hiley, Kulie, and Bennartz 2011). At lower latitudes there is higher likelihood of mixed precipitation, thus likely one of reason for an underestimation of snowfall. Hiley et al. (2011) admitted comparison with climatological, model-derived accumulations is not an optimal method of analyzing CloudSat retrievals, which is where ground-based observations serve as the best way to conduct such research. This, however, isn't a perfect comparison as there is not a universal method for a Z-S relationship, which is the relationship between radar reflectivity (Z) and snowfall rate (S), allowing for some uncertainty in these types of comparisons (Hiley, Kulie, and Bennartz 2011).

Another study conducted by Chen et al. (2016) used a Multi-Radar Multi-Sensor (MRMS/Q3) system to compare ground-based radar results to

CloudSat's retrievals. The authors found that over 99% of CloudSat surface snowfall events are greater than one kilometer above the surface, whereas over 75% of corresponding MRMS observations are below one kilometer to the near ground surface describing the difference in the lowest bin height for measuring reflectivity (Chen et al. 2016). Using the results from the MRMS, CloudSat overestimates light snowfall (<1 mmh^{-1}) and underestimates moderate (1-2.5 mmh^{-1}) and heavy snowfall (>2.5 mmh^{-1}) if gauge-adjusted operational scanning radar datasets are used as the baseline dataset for comparisons.

Other studies have also taken on the challenge of using a ground-based radar to compare CloudSat observations for snowfall rate. Norin et al. (2015) used the 2C-SNOW-PROFILE product from CloudSat to compare a network of ground-based radars in Sweden. The best agreement in results were when the snowfall rate had a range of $0.1 - 1.0$ mmh^{-1} and CloudSat took observations as it passed close (46-82 km) to a radar station in the network. Above that range, the 2C-SNOW-PROFILE has a limited ability to retrieve reliable observations (Norin et al. 2015). These results coincide with another study done by Cao et al. (2014), where the authors also used the 2C-SNOW-PROFILE product and compared the observed snowfall rates to those from the National Mosaic and Mulitsensor QPE System (NMQ) snowfall products. In general, results showed that CloudSat detected light snow (less than 1 mm hh^{-1}) well but above that level, detectability degrades relatively quickly (Cao et al. 2014). Both of these authors found results relating to snowfall rate that coincide with Chen et al. (2016). The previously mentioned CloudSat evaluation studies using ground-based radar highlight the complexity of comparing spaceborne with ground-based remote sensing datasets. They also hint at spaceborne detection deficiencies that can be further explored with ground-based radar datasets. Ground-based radar datasets like the Barrow, AK MMCR not only provide excellent evaluative datasets for current spaceborne platforms, but also provide valuable guidance for future spaceborne radar missions regarding the trade space between radar sensitivity and near-surface bin designation to effectively observe as much snowfall at the surface as possible.

The Global Precipitation Measurement (GPM) mission is the other current spaceborne precipitation measurement system. GPM succeeded the Tropical Rainfall Mission (TRMM) in 2014 as a joint mission between JAXA and NASA and provides precipitation measurements from its Dual-Frequency Precipitation Radar (DPR) and Microwave Imager (GMI) (Hou et al. 2014). As noted earlier, GPM has an orbital extent of $|65°|$ and a minimum DPR detectable reflectivity of 12 dBZ, which is limits its ability to measure light snowfall at extremely high latitudes like Barrow, AK, especially compared to CloudSat and its higher orbital pathway and increased radar sensitivity. As one of the current spaceborne precipitation measurement radars, it is relevant to compare to the potential results of this study.

2.2 Shallow Snowfall

Shallow snowfall is a key emphasis of this study and as mentioned earlier, the best way to observe snowfall, especially shallow snowfall, on a global scale is by using a spaceborne radar platform like CloudSat, due to it's low minimum detectable reflectivity and extended orbital extent. Shallow snowfall has multiple forms, where the term 'shallow' is most often defined as lower tropospheric cloud top heights. These shallow snowfall events occur throughout the world, but commonly occur near large bodies of water in the mid to high latitudes (Kulie et al. 2016). CloudSat is able to provide global snowfall observations and among it's product suite is the 2B-CLDCLASS, which is able to partition snowfall events into different types of snowfall regimes, which is conducted in Kulie et al. 2016. By utilizing this product, Kulie et al. (2016) found that about 95% of all snowfall cases could be partitioned into two cloud type categories, shallow cumuliform and nimbostratus. Figure 2.1 describes the relative frequency of cloud thickness for both categories. Shallow cumuliform being cumulus or stratocumulus clouds with generally very low cloud top heights and nimbostratus having a more even distribution ranging from low
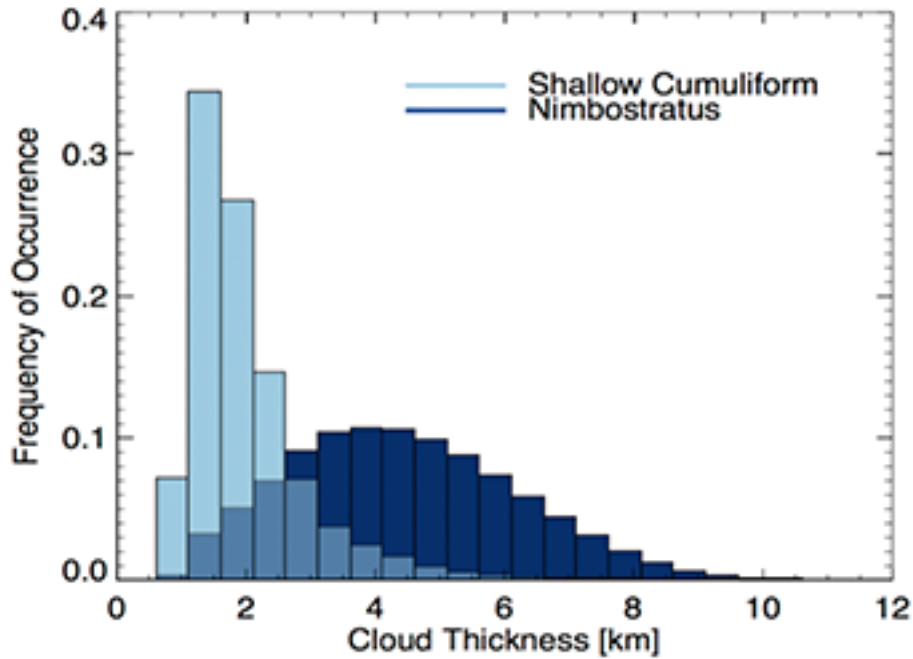
FIGURE 2.1: Relative frequency of occurrence of all snowfall, partitioned into two snowfall types, shallow cumuliform and nimbostratus, adapted from Kulie et al. (2016). This data is from the CloudSat 2B-CLDCLASS product from June 2006 to December 2010

cloud types from shallow events to deep cases with larger cloud top heights.

Recall Figure 2.2, which described CloudSat global snowfall observations and the respective snowfall fraction. Figure 2.3 is nearly the same figure, but is partitioned into each snowfall category and their respective snowfall fractions across the world. Overall, most of the world is dominated by nimbostratus snowfall, Figure 2.3b, however in the mid-latitudes, shallow cumuliform snowfall events, Figure 2.3a, tend to be the most common case. Throughout much of the Northern Hemisphere, about 40-50% of all snowfall events during this period are shallow cumuliform and specifically in Barrow, AK, about 30-40% of all snowfall was shallow cumuliform. Besides the areas at the edge of where snowfall actually occurs, in the lower mid-latitudes, about 60% of all snowfall observations being nimbostratus tends to be the average. Shallow snowfall is often too light and too low in terms of reflectivity and cloud top height respectively,
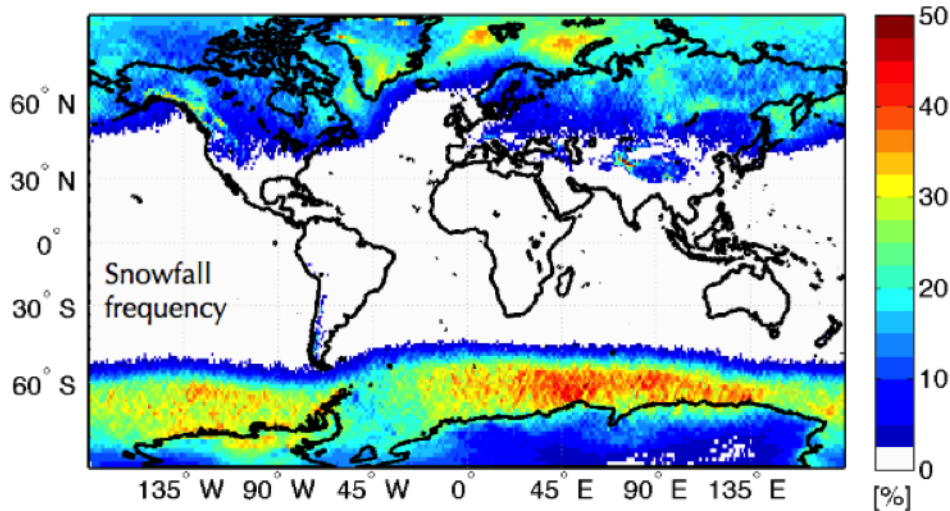
FIGURE 2.2: Relative frequency of occurrence of all snowfall, adapted from Kulie et al. (2016). This data is from the CloudSat 2C-SNOW-PROFILE product from June 2006 to December 2010
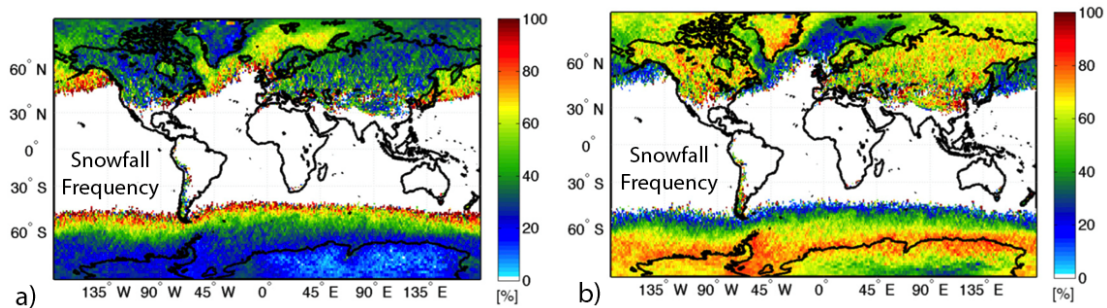
FIGURE 2.3: Relative frequency of occurrence of shallow cumuliform snowfall (a) and nimbostratus snowfall (b), adapted from Kulie et al. (2016). This data is from the CloudSat 2C-SNOW-PROFILE and CloudSat 2B-CLDCLASS products from June 2006 to December 2010

for satellite radar platforms to observe properly, which is why ground-based observations are important to use in order to study this phenomenon.

2.3 Atmospheric Radiation Measurement Climate Research Facility

The NSA Barrow facility features a 35 GHz Ka band (about 8 mm wavelength) Millimeter Wavelength Cloud Radar (MMCR) (Moran et al., 1998; Wang et

al., 2015). This MMCR is an unattended zenith (vertically) pointing ground-based radar that can provide reflectivity and vertical velocity data (Matrosov, Shupe, and Djalalova 2007). The minimum detectable reflectivity is -50 dBZ at a maximum cloud top height of five kilometers, but reflectivity profiles are available throughout the entire tropospheric depth with slightly higher minimum reflectivity thresholds, because Arctic environments like Barrow, AK are characterized by relatively shallow tropopause heights in the winter. Another useful tool of the MMCR is the measurement of cloud boundaries such as cloud bottoms or tops.

MMCR's were specifically designed to make long-term observations of non-precipitating and weakly precipitating clouds at Cloud and Radiation Testbed (CART) sites for the ARM program but can be used for precipitation retrievals like this research utilizes. There are only a handful of other MMCR's around the world, with some in the western Pacific, one in Oklahoma, and one in Greenland. They excel in regions where snowfall is the main form of precipitation because at the specific wavelengths of the MMCR, which are about an order of magnitude shorter than other storm surveillance radars like the NEXRAD WSR-88D that uses a 10 centimeter wavelength (S band), because ice crystals and snowfall produce minimal attenuation (Moran et al. 1998). The MMCR is an excellent tool to make the necessary measurements for this research. Ground-based radar datasets like the Barrow, AK MMCR not only provide excellent evaluative datasets for current spaceborne platforms, but also provide valuable guidance for future spaceborne radar missions regarding the trade space between radar sensitivity and near-surface bin designation to effectively observe as much snowfall at the surface as possible.

The other key instrument utilized for this study was the ARM Surface Meteorology Systems (MET). This instrument provided 1-minute observations of barometric pressure, surface wind speed, wind direction, air temperature, and relative humidity.

2.4 Area of Study – Barrow, Alaska

FIGURE 2.4: Satellite image of the ARM site location in relation to
Barrow, AK. Map Data ©2017 Google

The ARM site is located in Barrow, AK (71.32°N, 156.07°W, 8 m amsl), as shown in Figure 2.4. Barrow is the northernmost city is Alaska and the United States and is 330 miles north of the Artic Circle. The main shoreline of the city faces the northwest, as it is located on the western side of a rounded edge of land, with the NSA Barrow facility located northeast of the city. The Chukchi Sea on the western side and the Beaufort Sea on the eastern side surround Barrow to the north. The most significant geographical feature lies roughly 250 miles (about 400 km) to the south with the Brooks mountain range, where the largest peak reaches almost 9,000 ft. (2.7 km). This range can affect wind effect wind patterns through blocking southerly winds. Yearly temperatures average 17°F (-8°C) making it very cold year round and due to the extremely high latitude, daylight largely varies to each extreme. During the summer months there is entirely daylight and in the winter, there is little to no daylight making the normal diurnal cycle normally seen in the tropics and mid-latitudes non existent.

An interesting aspect when studying this region is that Barrow, AK is one of the most studied places on Earth to investigate the effects of climate change. Due to it's coastal exposure and low elevation that doesn't get much higher than 10 meters above sea level, the area is vulnerable to issues such as wind damage, erosion, and flooding, especially when exposed to extreme weather events (Cassano et al. 2006). An issue corresponding to climate change and the warming climate is the timing of the spring snowmelt, which affects hydrological and biological processes. One study has shown that the average date of the spring snowmelt has advanced by about 8 days since the mid-1960's (Stone et al. 2002). These results are related to the overall decrease in precipitation in this region despite an increase in annual temperature of about 1.6°C, which may be due to a multitude of reasons that may be correspond to the increase in temperatures (Stafford, Wendler, and Curtis 2000). Some possible causes include changes in wind patterns, variability in surface pressure, decreasing cloudiness, or a shift in the normal positions of the Aleutian low and Arctic high (Curtis et al. 1998). The aforementioned changes in climate for this region has lead to some changes in living for the residents of Barrow, AK. A couple examples are the changing sea ice conditions that affect whale harvests and wind conditions that becoming less suitable for hunting (Hansen et al. 2013). Policies and adaption for this region are important topics for this region as the changing climate has significant social and economic consequences (Stone et al. 2002; Lynch and Brunner 2007).

The motivation for this research is due to multiple scientific elements. Snowfall is important to the hydrological cycle of the Earth and serves as a key feature in sustaining human life. Also, improvement of spaceborne radar platforms for the future to obtain better and more reliable retrievals of snowfall is very important to the study of snowfall, and potential future changes in snowfall, on a global scale, especially in Arctic regions that frequently experience light snowfall events (Kulie and Bennartz 2009). Understanding the regional importance of different snowfall modes (e.g., shallow convective, deep synoptically forced, orographic, etc.) is also important from both a basic scientific and

spaceborne remote sensing perspective. Advancing the knowledge of the dependence snowfall has on various environmental parameters in a region that experiences shallow and light snowfall on a regular basis will greatly improve future forecasts and snowfall studies in general as well.

The primary goals of this study are:

- Investigating possible spaceborne radar biases in reflectivity profiles due to near-surface bin designation by analyzing ground-based radar datasets.

- Analyzing the possible consequences of the spaceborne detection blind zone and providing valuable snowfall detection guidance for future spaceborne radar platforms using ground-based profiling radar observations.

- Identifying the most common/rare snowfall regimes at NSA.

- Establishing the dependence of surface snowfall at Barrow, AK to environmental parameters (e.g., temperature, pressure, wind, sea ice cover, etc.).

- Quantifying snowfall rates and accumulation that are attributed to different regimes and parameters.

Chapter 3

Data

The dataset used in this study stems from two different sources. One of these sources is the ARM archive that provides all the data from the aforementioned MMCR and surface MET instruments, while the other source is the National Snow and Ice Data Center (NSIDC) archive, which provides global snow and ice coverage data. With these data sources, a seven year dataset was compiled from 2004-2011. This section provides a brief overview of each data source and the methodology used to merge each relevant parameter.

Using the ARM archive, the reflectivity and vertical velocity data were gathered from 15 April 2004 to 23 March 2011 in order to determine whether this site was suitable for a potential study. The following data stream was used for study: North Slope Alaska, Central Facility Barrow, AK, MMCR radar moments product (nsammcrmom.C1.b1). Only mode 4 (precipitation mode) MMCR profiles were used for the following analysis. To separate the data year by year, annual data periods were defined from July to July, except for 2004 and 2011 that contained partial years due to the previously described dataset start and stop dates. This means a year of data considered for 2006-2007, for example, stretches from July 2006 to the end of June 2007 to ensure all of the winter and colder temperatures are taken into account in each boreal winter.

The reflectivity and cloud boundary data were the most important parameters to analyze since both were predominantly used throughout the research process. The MMCR at NSA has an excellent sampling rate of nine seconds. There were some major observational data gaps due to abnormally high reflectivity signatures that were deemed untrustworthy during these periods:

December, 2007, January 2008, 1-13 February, 2008, 10-18 January, 2010, and 10-23 February, 2010. The vertical data bin was also different during two periods of the dataset. From the beginning of the dataset in early 2004 to 13 December, 2007, the vertical data bin encompassed levels from 157 meters to just over 10.0 kilometers. From that time on until the end of the dataset in early 2011 the vertical data bin went from 140 meters to 9.76 kilometers. The near-surface radar bin height is 157 meters and 140 meters for these two time periods, which was defined as the assumed surface for any snowfall rate calculations, as it was the lowest height bin possible to make these types of measurements. For each period, data bin spacing was 90 meters and 87 meters, respectively. Cloud boundaries for each MMCR profile were defined as layers consisting of at least one radar reflectivity value exceeding -45 dBZ. Distinct cloud layers were defined if reflectivity gaps in the profile exceeded an ad hoc 5 data bin (215 m) threshold. Cloud boundary number and heights of each respective layer were also retained.

This dataset was then divided into three different surface precipitation regimes: snowfall, mixed precipitation and rain. Each was separated by a temperature range where each respective form of precipitation is most likely to exist. A probable precipitation event in the initial databases was defined as any MMCR near-surface reflectivity exceeding -30 dBZ. This reflectivity precipitation event threshold was further refined in later stages to conform with spaceborne snowfall/precipitation datasets (e.g., CloudSat uses a -15 dBZ threshold to define probable surface snowfall events).

Surface MET instrument observations from the ARM-standard Meteorological Instrumentation at the Surface data stream (nsamet.C1.b1) were also merged with MMCR radar observations. From this instrument, one minute statistics of various environmental parameters such as barometric pressure, two meter temperature, relative humidity, wind speed, and wind direction data from the surface MET files were read. These were then interpolated from the present weather sensor and detectors (PWS and PWD) using standard UTC time to

match the MMCR time and standardize the merged dataset. In total, this dataset includes over ten usable parameters just from the ARM archive data. A NSA MMCR snowfall dataset was defined as any probable precipitation event that accompanied a 2 m temperature below 2°C. The 2°C value conforms to observational studies that indicate a 50% snow probability associated with this temperature threshold (Liu 2008). A separate mixed precipitation dataset was also created and populated with any probable precipitation observation with a 2 m temperature between 0°C and 2°C. Similarly, any probable MMCR-defined precipitation events occurring with a 2 m temperature above 2°C was considered rainfall.

3.1 Data Content

	04-11	2004	2005	2006	2007	2008	2009	2010	2011
■ Snow	80.7%	73.4%	77.0%	77.9%	97.2%	76.2%	82.3%	80.4%	100.0%
■ Rain	11.2%	17.9%	13.7%	16.2%	1.7%	11.6%	9.9%	12.9%	0.0%
■ Mixed	8.0%	8.7%	9.3%	5.9%	1.1%	12.2%	7.8%	6.8%	0.0%
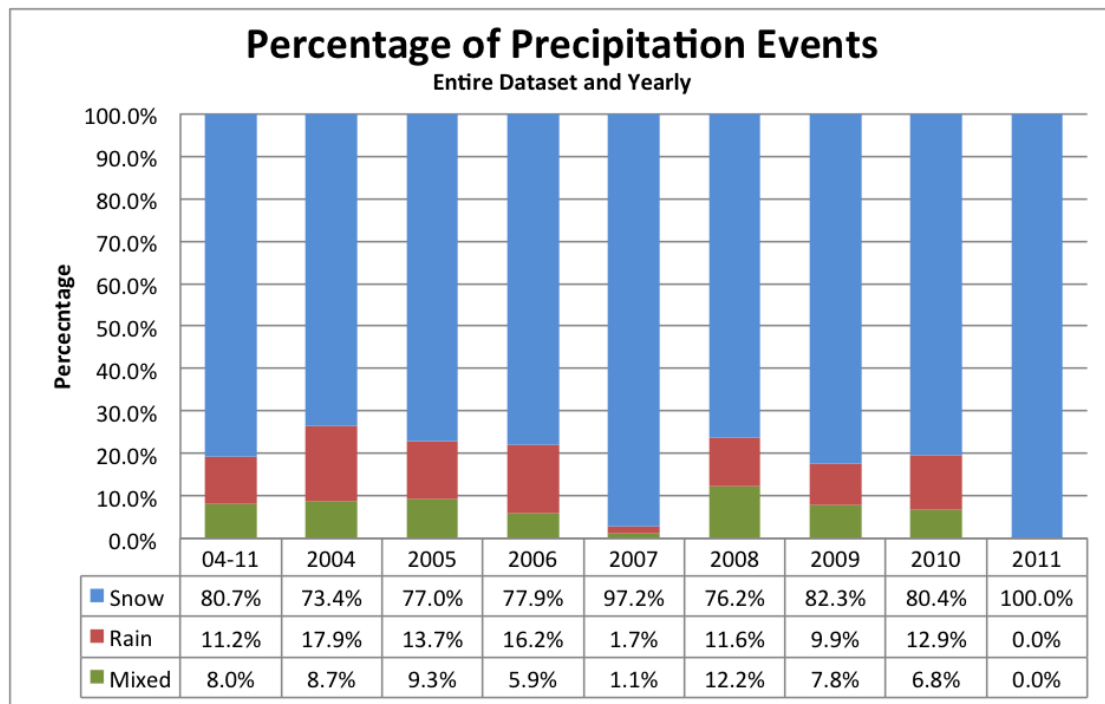
FIGURE 3.1: Percentage of precipitation events for the entire dataset based on amount of data points in each of the three precipitation categories, snow, mixed precipitation, and rain, separated by year

Using defined temperature thresholds to separate the three precipitation types, the majority of the precipitation events were snowfall events at just over 80%
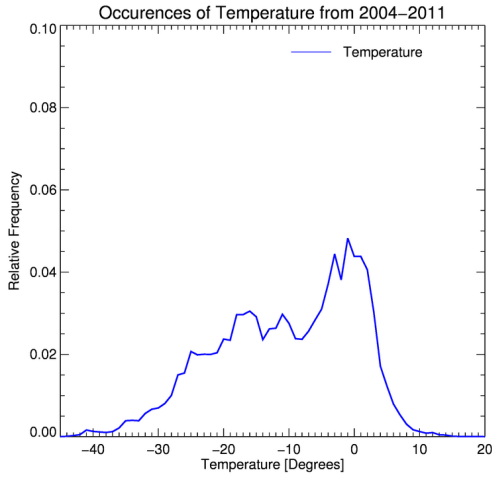
FIGURE 3.2: Relative frequency of occurrence of temperature for the entire dataset, for each of the three categories of precipitation separated by their respective temperature thresholds
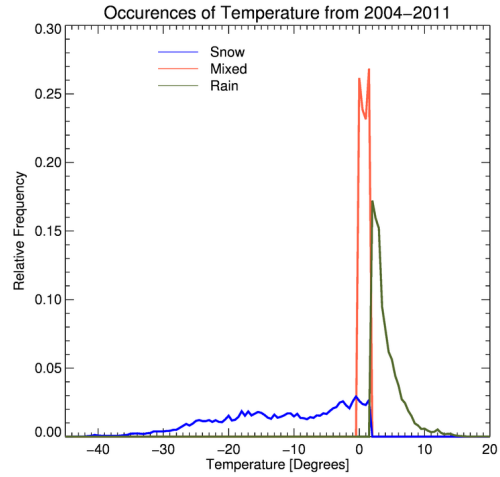
FIGURE 3.3: Relative frequency of occurrence of temperature for the entire dataset, for each of the three categories of precipitation separated by their respective temperature thresholds
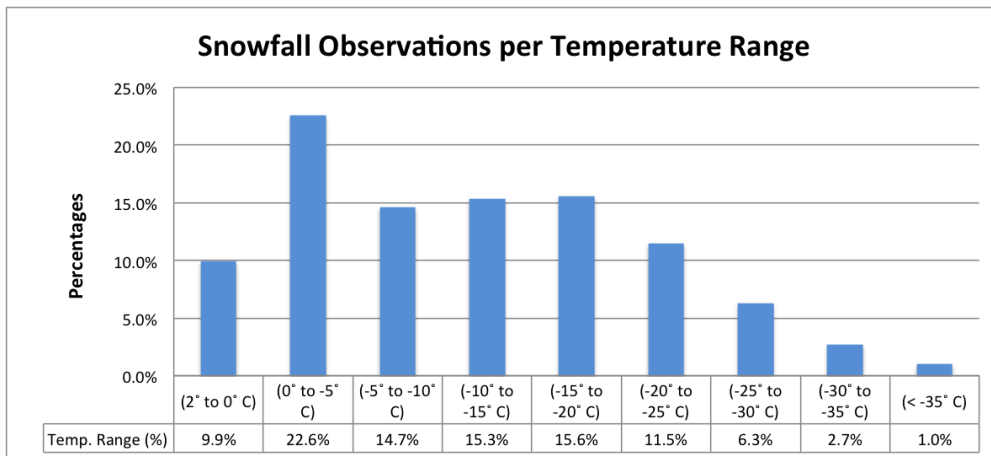
FIGURE 3.4: Percentage of snowfall observations per temperature range where each range is separated by increments of 5°C except for 2° to 0°C thresholds

as shown in Figure 3.1. Rainfall events and mixed precipitation events occur 11.2% and 8% of the time respectively. A similar trend exists every year except 2008, where there are more rainfall events than precipitation events. The data from 2011 only goes to late March, hence the lack of mixed precipitation and rainfall events.

The temperature at which precipitation events occur most often are shown in

Figure 3.2. The highest relative frequency of occurrence ranges from about -3°C to 3°C and most observations are below that 3°C threshold. Figure 3.3 describes the relative frequency of occurrence for each respective precipitation type. There is a relatively even distribution for snowfall events, although the relative frequency decreases slightly with decreased temperature. The mixed precipitation range is small causing an even distribution and the rainfall events sharply decrease in relative frequency with increased temperature. Snowfall is the predominant focus of this study so analyzing the amount of events that fall into certain ranges is of interest as shown in Figure 3.4. The majority of snowfall events occur with higher temperatures, especially above -20°C, with the 0° to -5°C range having the most events at just over 22%.

From the reflectivity observations, snowfall rates were calculated and then added to the merged radar/MET dataset. Since the MMCR is a pulsed system, a Z_e-S relationship for dry snow under a basic set of combined snowflake backscatter assumptions for millimeter wavelengths and microphysical properties (e.g, assumed snowflake size distribution) is used to derive instantaneous snowfall rates [mmh^{-1}] according to $Z_e = 56\,S^{1.20}$ (Castellani et al. 2015; Matrosov, Shupe, and Djalalova 2007). Radar accumulation was also included in the final merged dataset by multiplying the instantaneous radar-derived snowfall rate by the time [hours] increment between successive radar scans. This process turns the initial measured snowfall rate in mmh^{-1} to mm. A maximum time increment of five minutes was adopted if data gaps existed in the MMCR dataset. Typical times gaps exist between consecutive radar scars on the order 10-15 seconds. Once again, a maximum of 5 minutes was induced if there was an extended radar gap longer than this time interval.

The final resource employed was gridded snow and sea ice coverage data via the NSIDC archive. The product used was the Near-Real-Time SSM/I-SSMIS EASE-Grid Daily Global Ice Concentration and Snow Extent, Version 4 (NISE).

The NISE snow and sea ice algorithm both use near-real-time brightness temperature observations that originate from the SSMIS instrument on the DMSP-F17 satellite. Sea ice concentration percentage is derived using the NASA Team total sea ice algorithm. Snow extent is mapped separately using an algorithm developed for Scanning Multichannel Microwave Radiometer (SMMR) data and modified for use with SSM/I data (Nolin, Armstrong, and Maslanik 1998). This data provides the fraction of snow and ice coverage for multiple grid boxes out to five degrees latitude/longitude. Once gathered, these data files were then be merged into larger dataset, to create one large dataset that would serve all the needs of this research.

Chapter 4

Methodology

In order to gain the most basic knowledge of the NSA site at Barrow, AK before attempting to accomplish the primary goals of the research, daily reflectivity and vertical velocity profiles were created via the seven year dataset from the ARM archive (www.archive.arm.gov). This step provided a valuable overall sense of the various snowfall regimes that occur at this unique Arctic site. The next logical step was to create aggregated contoured frequency by altitude diagrams (CFAD), which show two-dimensional joint histograms of radar reflectivity observations as a function of their respective cloud top height. CFADs will be used to show all observations for the entire dataset based on two very relevant variables and can be further parsed into separate years to show yearly variability and what types of snowfall are most common. To enhance this information, multiple statistics for total snowfall and accumulation occurrences were gathered based on various reflectivity and cloud level thresholds.

In order to study possible spaceborne radar biases, reflectivity correlation plots were the next research step. The vertical reflectivity correlations between the MMCR lowest usable data bin (about 140 meters above ground level) and all levels below two kilometers were taken for various cloud top height (CTH) thresholds (e.g., CTH less than 1, 1.5, 2, and 4 km, as well as CTH greater than 6 kilometers). Vertical reflectivity analysis was also performed on the entire snowfall dataset in order to compare the differences between the multiple snowfall regimes. Along with studying spaceborne radar biases, another primary goal of this research is determining what current and future spaceborne radar platforms may miss given certain thresholds of minimum

detectable reflectivity and cloud top height. To analyze this aspect, various statistics were created in order to determine what percentage of snowfall observations would be missed given the aforementioned thresholds.

The next primary goal of this research is to investigate environmental parameters to study the dependence of snowfall at Barrow, AK for these various parameters. To conduct this part of the research, one and two dimensional histograms, which show the relative frequency of occurrence multiple parameters, were utilized to create as many combinations of environmental parameters as possible. This contributes even more information the established knowledge of snowfall at NSA. Among the histograms showing environmental parameters, snowfall rate is also studied in accordance with other environmental parameters to accomplish a similar goal of determining what snowfall rates correspond to certain thresholds of pressure and cloud top height for example.

Since Barrow, AK is located on the Arctic Ocean coastline in northern Alaska and is therefore influenced by this large body of water, the last step in this research incorporated the ocean ice fraction data over from the NSIDC. The ocean ice fraction considers any data from a 5 degree area centered on the ARM site. Incorporating and then analyzing the ocean ice fraction data requires going back to earlier steps and using information from figures like the total dataset CFAD or various histograms into two comparative collections, one showing the same data where ice was present and one showing data where no ice was present. Identifying the effects of ice coverage on snowfall and its implications on various parameters and snowfall, in general, further reinforces the knowledge of precipitation at NSA.

Chapter 5

Results

5.1 North Slope Alaska Profile

To investigate observations on a daily scale and illustrate common snowfall modes observed by the MMCR at the NSA site, two days with a full 24 hours reflectivity associated with snowfall events are first shown as examples. Figure 5.1 shows the reflectivity (dBZ) at a given altitude (km) and time of day (hours) for 13 October 2004 (a) and 22 February 2008 (b), respectively. In Figure 5.1a, the entire period shows cloud top heights (CTH's) at around 1 km with varying light reflectivity values at or below 0 dBZ. The entire day has very light precipitation and shallow clouds, which is a common occurrence at NSA (Shupe et al. 2008; Wang, Geerts, and Chen 2015). On the opposite end of the spectrum, Figure 5.1b shows deeper CTH's just less than 8 km and much higher reflectivities throughout the profile with some surface values reaching 15 dBZ. These two cases show snowfall events forced and sustained by different mechanisms and nicely illustrate the snowfall mode variability at NSA.
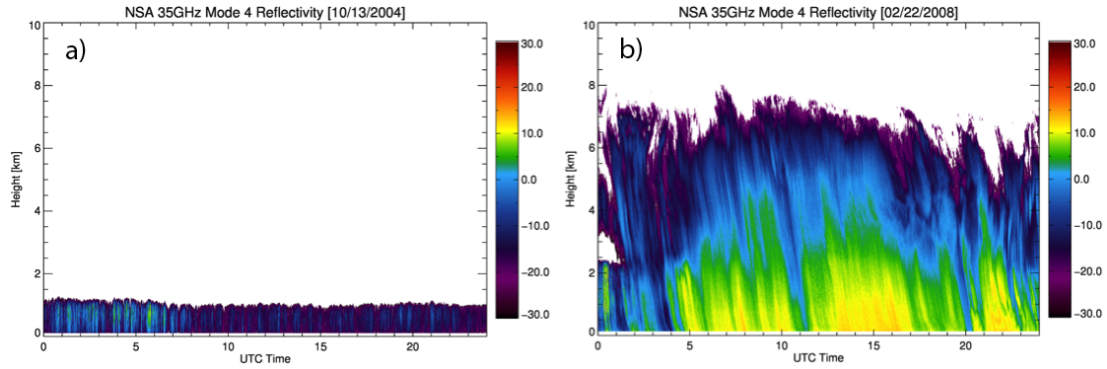
FIGURE 5.1: Daily reflectivity from NSA 35GHz radar with UTC time and height [km] for October 13 2004(a) and February 22 2008(b)

In the week surrounding 13 October 2004, average temperatures were 22°F (-5.6°C) and a low pressure system was moving into the region. On 13 October 2004, relative humidities were above 80% throughout the entire day, peaking in the low 90's. Pressure was relatively high at about 1022 hPa, and temperatures ranged from 19.9°F (-7.2°C) to 22.1°F (-5.6°C). The wind was a strong eastern 21 mph (34 kmh^{-1}) wind and was consistent throughout the entire day. Ice coverage in the region around Barrow was at about 48% during this time of the year. The second case, the week of 22 February 2008 had average temperatures of 0°F (-18°C) and was in the midst of a low pressure system. Pressures started to climb toward the end of the week, starting the 22nd where measured pressures were 988 hPa at the start of the day before rising to 1000 hPa to conclude the day. Temperatures varied throughout the day as there was a low of 8.6°F (-13°C) and a high of 19.9°F (-7°C). The wind in the morning was from the south before transitioning to the northwest in the early afternoon, which coincided with the increasing temperatures and amplifying wind speed from a calm 5-10 mph (8-16 kmh^{-1}) wind in the morning to a strong 15-20 mph (24-32 kmh^{-1}) wind at night. The surrounding ocean was also fully ice covered.
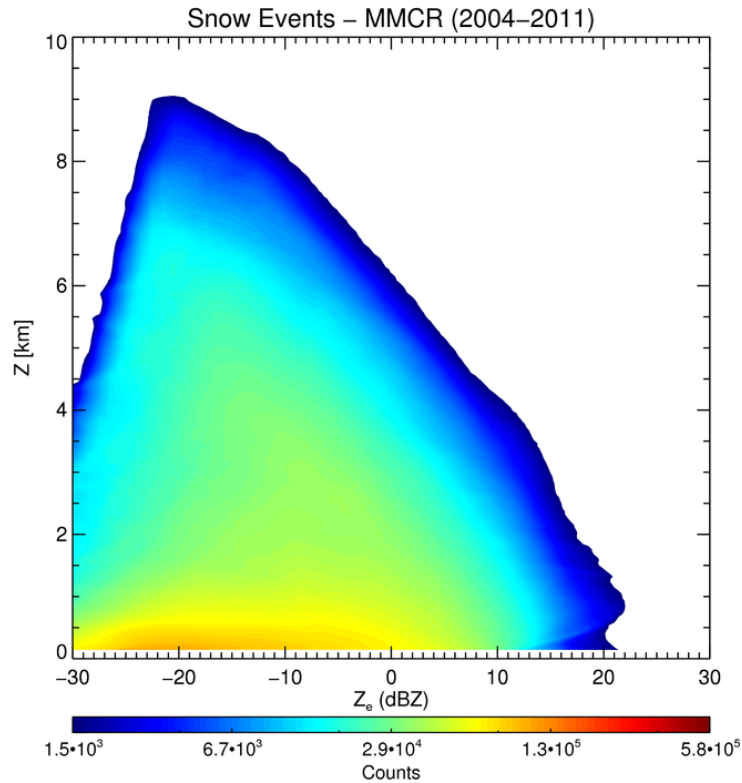
FIGURE 5.2: Contoured frequency by altitude diagram (CFAD) displaying the total number of snowfall observations for MMCR reflectivity versus cloud top height for the entire dataset from 2004 to 2011

Figure 5.2 shows a joint two-dimensional histogram of MMCR snowfall observation data points given their respective reflectivity (dBZ) and altitude (km) from the entire 2004-2011 MMCR dataset, which once again consists of over four million data points. This figure helps describe the overall characteristics in snowfall events and illustrates the types of snowfall are most common or rare in Barrow, AK. It also allows one to view the entire dataset as controlled by two the most relevant parameters, reflectivity and altitude. Overall, the entire dataset extends past both reflectivity limits of -30 and 20+ dBZ and shows a maximum CTH of just over 9 km. The majority of the observations fall between about -30 and 15 dBZ and below about 7 km, with the highest number of observed counts between -25 and 5 dBZ and less than 1 km. These characteristics represent the fact that most of the NSA MMCR snowfall observations are both shallow and relatively light in intensity.
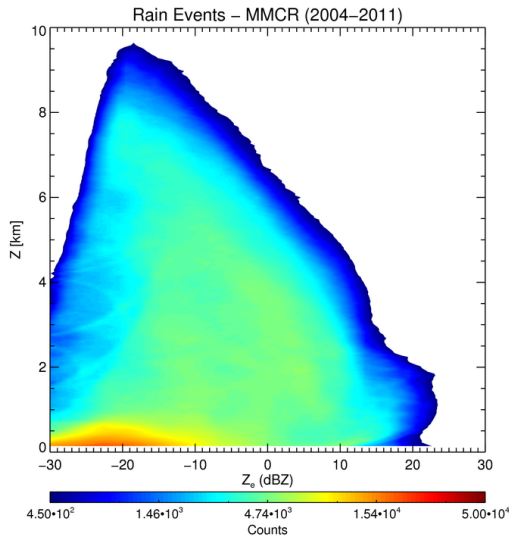
FIGURE 5.3: Same as Figure 5.2, but for the total number of rainfall observations
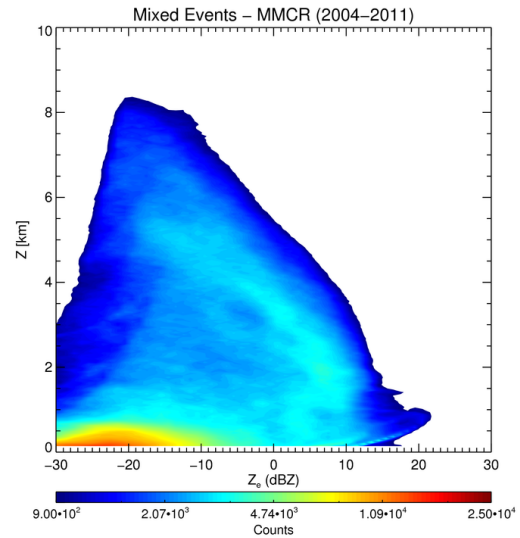
FIGURE 5.4: Same as Figure 5.2, but for the total number of mixed observations

Along with the snowfall observation, the entire dataset of possible mixed precipitation observation and probable rainfall observations can be shown in the same way as a function of height and reflectivity via Figures 5.3 and 5.4. This allows one to view the dataset in three separate precipitation types in order to see if there are different reflectivity or CTH trends throughout each type. Overall, there are much less observed counts of mixed precipitation, about 400,000 or 8% of all probable precipitation cases, compared to snowfall events and rainfall observations, which accounts for about 600,000 or 11% of all probable precipitation cases, however characteristics can still be analyzed. Very similar to the previous figure showing the entire snowfall observation dataset, the majority of observed counts are located at very shallow CTH's and very light reflectivities at less than 1 km and between -30 and -10 dBZ, respectively. The majority of light reflectivity observations has shifted slightly to lower reflectivities in comparison to the snowfall dataset. In general, throughout all three precipitation partitions of the entire dataset show the same trend of very shallow CTH's and light reflectivities being the common observations seen at NSA.

As Figures 5.5 and 5.6 show, there is not only variability on a daily scale, but also on a yearly scale. Each of those figures show the same items, however
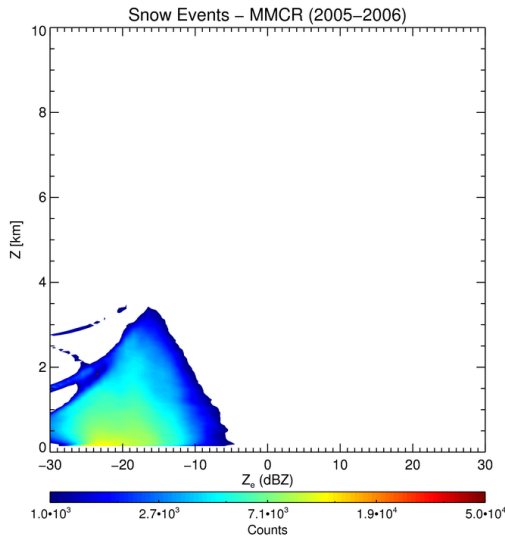
FIGURE 5.5: CFAD displaying the total number of snowfall observations for MMCR reflectivity versus cloud top height for the 2005 to 2006
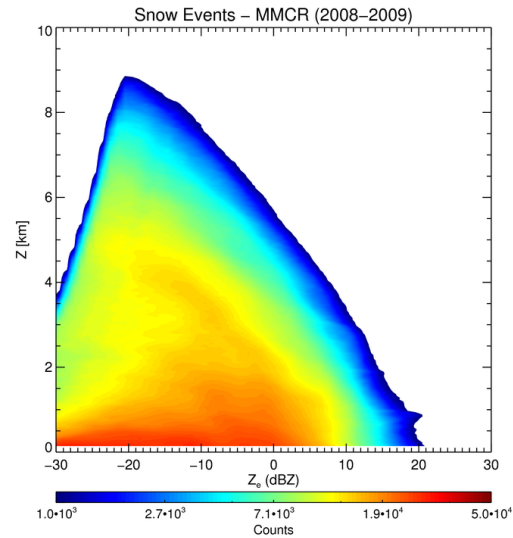
FIGURE 5.6: CFAD displaying the total number of snowfall observations for MMCR reflectivity versus cloud top height for the 2008 to 2009

instead of all snowfall observations across the entire seven year dataset, these show all of the snowfall observations for just two separate years of the entire seven year dataset in order to breakdown this dataset even further. Recall that annual results are presented by pre-defined snowfall seasons that extend from July to June, thus capturing the characteristics of each boreal winter. Figure 5.5 shows all snowfall observations from 2005-2006 and Figure 5.6 shows all data from 2008-2009. In total, there are many less snowfall observations in 2005-2006 than 2008-2009, which is a much more robust yearly dataset. Nearly all of the NSA MMCR observations in 2005-2006, Figure 5.5, are less than 2 km and less than -5 dBZ, so there were very light reflectivities and very shallow CTH's for almost the entire year, whereas in 2008-2009 the data is much more dispersed and indicates a mixture of snowfall modes. The majority of 2008-2009 snowfall observations are between -30 dBZ and 10 dBZ in reflectivity and less than 2 km in CTH, thus suggesting a prominent shallow snowfall signature. Note, however, that a distinctive deeper snowfall mode also exists for the 2008-2009 season, whereby MMCR reflectivity steadily increases with decreasing height. The axis of this deeper snowfall mode appears near 5 km and shows notable reflectivity enhancements below 3 km.
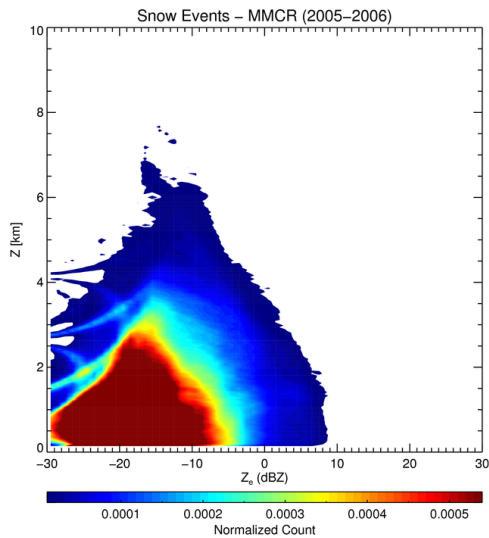
FIGURE 5.7: CFAD displaying normalized snowfall observations for MMCR reflectivity versus cloud top height from 2005 to 2006
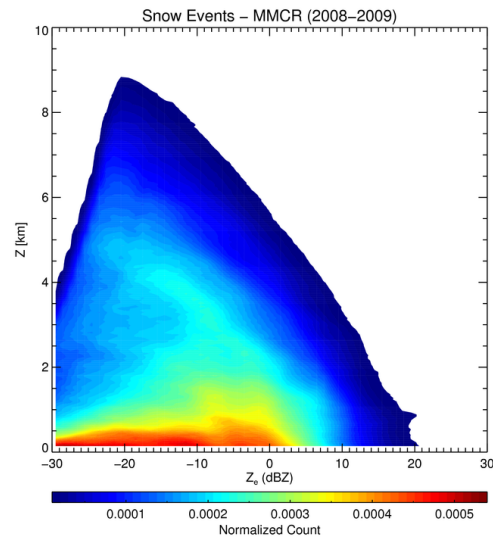
FIGURE 5.8: CFAD displaying normalized snowfall observations for MMCR reflectivity versus cloud top height from 2008 to 2009

To gather a clearer comparison between the two years, Figures 5.7 and 5.8 show the normalized count of snowfall observations in order to better compare seasonal results. The normalized count was tabulated by taking the number of observations in a given height and reflectivity bin. The number of observations found in each bin was then divided by the number of observations across the entire dataset, which therefore means that the sum of the entire plot is equivalent to one. The normalized count allows for a greater emphasis on the region in the plot where snowfall observations occur most often and creates an easier comparison between the two years of data since the results are presented in a normalized fractional form. In 2005-2006, as shown in Figure 5.7, similar to the earlier figure (5.5) showing all observed snowfall counts, almost the entire year of data are below 5 dBZ and 5 km in CTH with the highest normalized counts being below -10 dBZ and 3 km. Once again, the entire year of snowfall data is incredibly light and shallow.

In direct comparison, 2008-2009 features a much larger set of snowfall observations. (Figure 5.6) 2008-2009 exhibits similar characteristics as Figure 5.2, the entire seven year dataset, in terms of the distribution of snowfall observations. Reflectivity for this year stretches from -30 to 20 dBZ and the maximum CTH is

nearly 9 km. Never-the-less, a majority of normalized counts fall below 2 km in CTH. While there are many more normalized counts at higher reflectivities in 2008-2009 compared to 2005-2006, overall the two years of observations share the same commonalities in that very shallow and light reflectivities represent the predominant region of highest normalized counts.

5.1 North Slope Alaska Profile – Section Summary

- Shallow and light snowfall events are the predominant regime at NSA

- Significant daily and yearly variability

- Rain and mixed precipitation events have a similar distribution in terms of reflectivity and cloud level

5.2   Key Statistics

- Cloud Top Height, Reflectivity, Accumulation

In order to better assess the entire dataset of snowfall observations with respect to reflectivity (Z) and CTH occurrence, statistics based on certain Z/CTH thresholds were calculated as shown in Figure 5.9. This type of analysis quantitatively describes the most common snowfall regimes and highlights potential spaceborne radar detection issues associated with different snowfall regimes given the specific thresholds. To better understand this figure, the far bottom right red pixel, means that about 48% of all snowfall observations (any observation with reflectivities above -30 dBZ) were less than 6 km in CTH, but also greater than -15 dBZ for the reflectivity. Each pixel represents the percentage of snowfall observations that occur given the two thresholds of CTH and reflectivity.
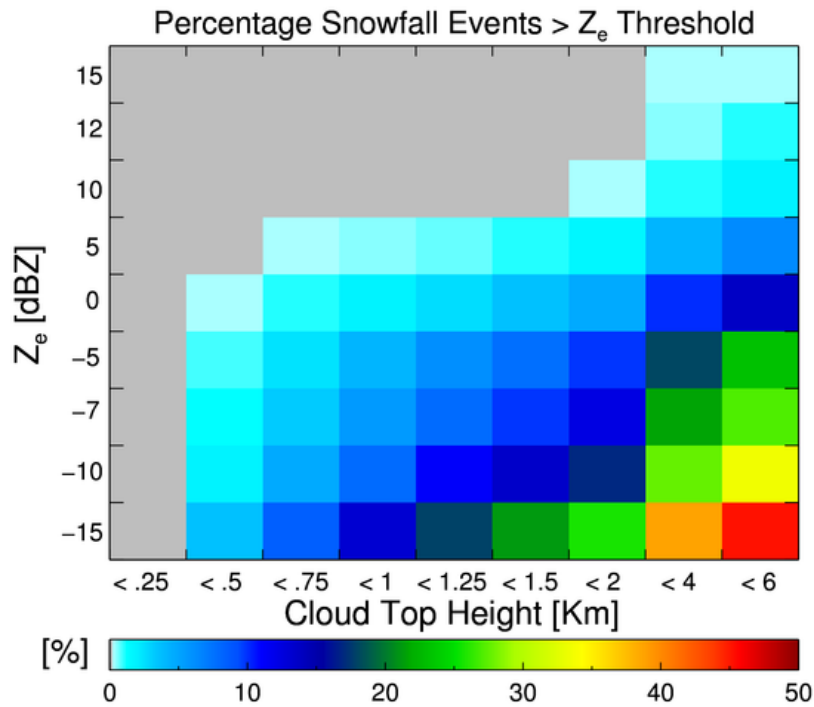
FIGURE 5.9: The percentage of snowfall events at certain minimum reflectivity thresholds versus cloud top height using the entire MMCR dataset

These statistics provide extremely valuable snowfall detection guidance regarding their given minimum thresholds for identifying snowfall and precipitation in general. The first current spaceborne radar that will be examined is CloudSat. Over land surfaces, CloudSat uses a near surface bin located near 1 km above ground level (AGL) to safely avoid ground clutter issues, where the profile below 1 km is referred to as the spaceborne blind zone. In this blindzone, roughly 50% of observed snowfall occurrence are below this level. However, using CloudSat's 2C-SNOW-PROFILE product, which determines "snow certain" precipitation to be any near surface reflectivity above -7 dBZ. Given the appropriate environmental parameters, it can be determined that about 6% of all snowfall observations were above -7 dBZ but also below 1 km, which would be directly in CloudSat's blindzone. This means that about 6% of all snowfall observations that were deemed snow certain, would most likely be missed by CloudSat. Taking these results and comparing them to the 2005-2006 year of data, Figures 5.5 and 5.7, where almost all of the snowfall observations

from that year were below -7 dBZ, CloudSat misses almost an entire year of data given these two thresholds. CloudSat also utilizes a threshold of -15 dBZ to determine any near surface observation as a near probable snowfall event. Performing a similar analysis to determine the percentage of occurrences that are above -15 dBZ but below 1 km, about 13% of all snowfall probable classified observations would be directly CloudSat's blindzone.
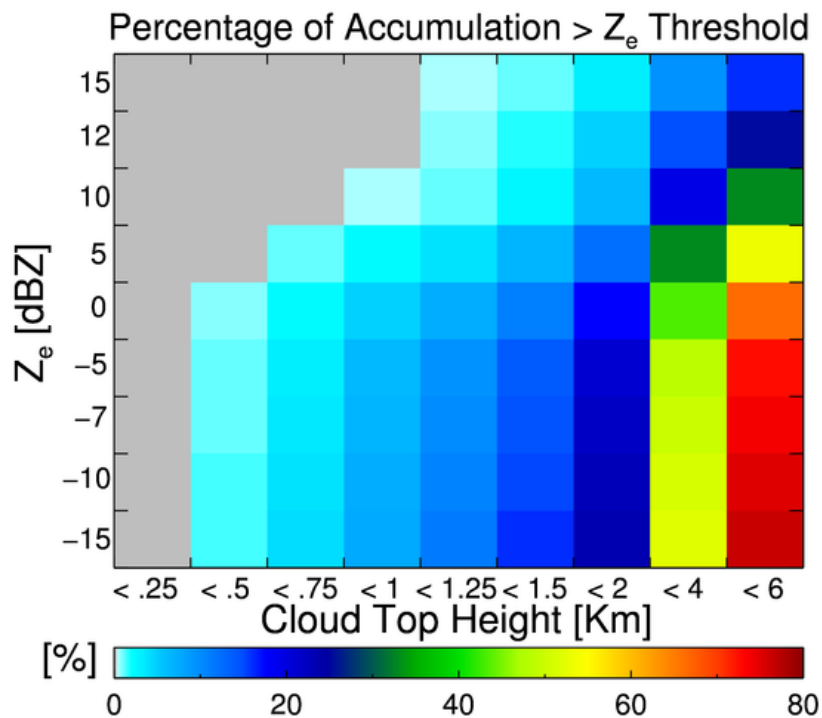
FIGURE 5.10: The percentage of accumulation occurrences at certain minimum reflectivity thresholds versus cloud top height using the entire MMCR dataset

The statistics shown are especially valuable when combined with accumulation statistics that are within the same thresholds as shown in Figure 5.10. Once again, accumulation statistics were based on taking the snowfall rate from the following Z-S relationship, $Z_e = 56\ S^{1.20}$, and multiplying that by the time increment between successive radar scans. Over 76% of snowfall accumulation derives from events with reflectivities greater than -15 dBZ and cloud top heights are lower than 6 km. Comparing the previous relevant reflectivity thresholds for CloudSat, 7% of all accumulation are in CloudSat's snow certain

threshold (-7 dBZ) and 8% of all accumulation occurrences are in CloudSat's snow probable threshold (-15 dBZ). Overall, about 6% of all accumulation comes from events that reside entirely within CloudSat's blindzone of less than 1 km with no reflectivity thresholds included.
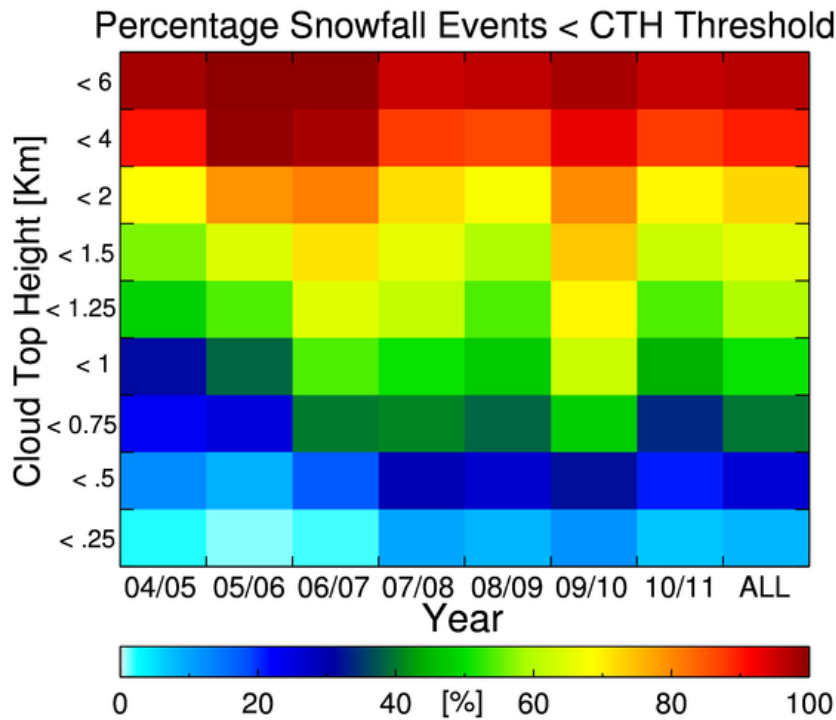
FIGURE 5.11: The percentage of snowfall events at certain cloud top height thresholds for years of data versus cloud top height

The next set of statistics uses the number of observations with multiple cloud top thresholds for each year of data and the entire dataset, which is shown in Figure 5.11. From this analysis, which can be combined with the accumulation statistics shown in Figure 5.12, can describe the estimated number of snowfall events missed by spaceborne radars if they could not detect below certain CTH levels creating blindzones can be calculated. Figure 5.11 also provides a better sense of the yearly CTH variability associated with snowfall. The year to year variability is an obvious feature of Figure 5.11. In 2005-2006 and 2006-2007, most the the observations fall below 4 km, whereas years like 2008-2009 and 2010-2011 have many more deeper cases of snowfall. Inspecting the far right column of the figure, which describes the data from the entire dataset, one
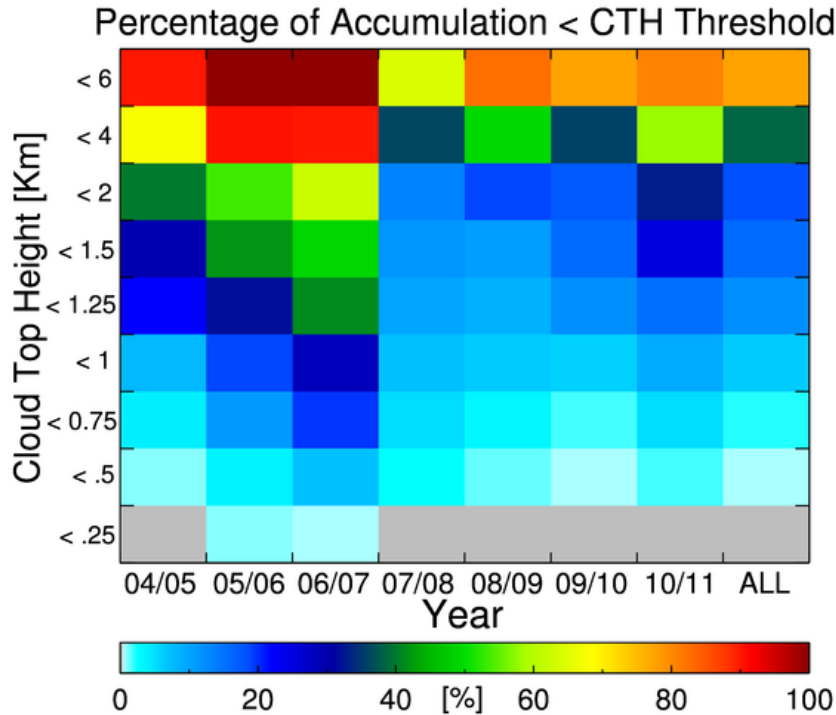
FIGURE 5.12: The percentage of accumulation occurrences at certain cloud top height thresholds for years of data versus cloud top height

can use these statistics to infer how many snowfall observations would be missed at certain CTH threshold. Using these statistics shows that 73% of all snowfall occurrence observations fell below 2 km in CTH, which accounts for 18% of all accumulation and 50% of all snowfall observations fell below 1 km, which accounts for just over 6% of all total accumulation. Once again, comparing to the current spaceborne radar of CloudSat, the lowest usable bin is about 1 km AGL over land, so potentially half of all snowfall occurrences or over 6% of total snowfall accumulation occurrences at the NSA site could be missed. It is important to stress these results as the employment of these statistics could improve spaceborne radar platform results, especially in other middle to high latitude regions that experience similar snowfall patterns of light reflectivity and shallow CTH's on a regular basis. It should also be noted that further spatiotemporal averaging should be performed to provide more realistic percentages (e.g., no temporal averaging or profile averaging to better mimic the sampling characteristics of a spaceborne radar was performed).

Moving to another current precipitation measuring spaceborne radar, the Global Precipitation Mission (GPM) has a radar with a minimum detectable reflectivity of about 12 dBZ. Using the same statistics, about 98% of all snowfall observations fall below 12 dBZ and would be missed by a GPM-like sensor, if it measured into the higher latitudes. 39% of total snowfall accumulation occurs at reflectivity above 12 dBZ, however these occur with higher CTH's as less than 1% of all accumulation occurrences are greater than 12 dBZ and directly in the blindzone of less than 1 km. These statistics can also be valuable to future missions that work with precipitation measuring spaceborne radars.

A future mission currently in preparation is the Aerosol/Clouds/Ecosystem (ACE) Mission, which will be another satellite radar platform capable of measuring precipitation from space. This mission plans to feature a minimum detectable reflectivity of 0 dBZ. Only about 16% of all snowfall observations were above this level, but only 2% of of these were below 1 km, assuming the same blindzone threshold of 1 km. This means about 84% of all snowfall observations would be missed. On the accumulation side, almost 89% of all accumulation observations are above 0 dBZ, since most accumulation occurs at higher reflectivities, so this spaceborne radar would likely be more applicable for observing accumulation rather than snowfall events, in place where light and shallow snowfall events occur often.

There are some other relevant thresholds to consider for potential spaceborne radars. For example, if the minimum detectable reflectivity is set at -10 dBZ, 36% of total snowfall occurrences and 98% of total accumulation occurrences are above -10 dBZ, so once again, this setting would capture the majority of accumulation, but miss almost two thirds of all snowfall occurrences. At a minimum detectable reflectivity of -5 dBZ, 32% of total accumulation occurrences and 95% of total accumulation occurrences are above -5 dBZ. Another aspect to consider is a decreased blindzone, with the same snow probable threshold as CloudSat (-15 dBZ). If the blindzone were decreased to 750 m, 500 m, or

even 250 m the amount of snowfall observations missed would decrease from 50% at 1 km to 40%, 26%, and 9% for each blindzone level previously listed respectively. Given CloudSat's current capabilities for measuring snowfall, identifying a way to decrease the blindzone can significantly increase the amount of snowfall events observed and measured.

5.2 Key Statistics – Section Summary

- 6% and 13% of total snowfall occurrences that fall within CloudSat's snow certain and snow probable criteria, respectively, are directly in the blindzone of 1 km. This equates to 7% and 8% of total accumulation occurrences at the same thresholds.

- 73% and 50% of total snowfall occurrences fall below 2 km and 1 km cloud level. This equates to 18% and 6% of total accumulation occurrences at the same thresholds.

- GPM's minimum detectable reflectivity of 12 dBZ would miss about 98% of snowfall observations at NSA, contributing to 60% of total accumulation occurrences if it measured at that latitude.

- A minimum detectable reflectivity of 0 dBZ would miss 84% of snowfall observation at NSA, contributing to 11% of total accumulation occurrences at NSA if applied to a future spaceborne radar platform.

- Future spaceborne radar platforms need to identify ways to decrease the blindzone, as that could have the greatest impact in improving surface snowfall detection. If the blindzone were to be decreased by half, from 1 km to 500 m, the amount of snowfall observations missed at NSA could be nearly halved.

5.3   Investigation of Spaceborne Radar Bias

To correspond with the blindzone analysis, correlations between reflectivity values at the lowest usable MMCR data bin located 125 AGL compared to every value above it were taken at multiple CTH levels, as shown in Figure 5.13. Note that native MMCR profiles are used so no spatiotemporal averaging was performed to generate the statistics provided in this section. Figure 5.13 shows correlations below 2 km because, as stated earlier, just over half of all snowfall observations fell below that 2 km level. The lowest MMCR usable bin serves as a proxy for surface conditions – a much more realistic proxy compared to the typical 1 km AGL level used by current spaceborne sensors over land surfaces.
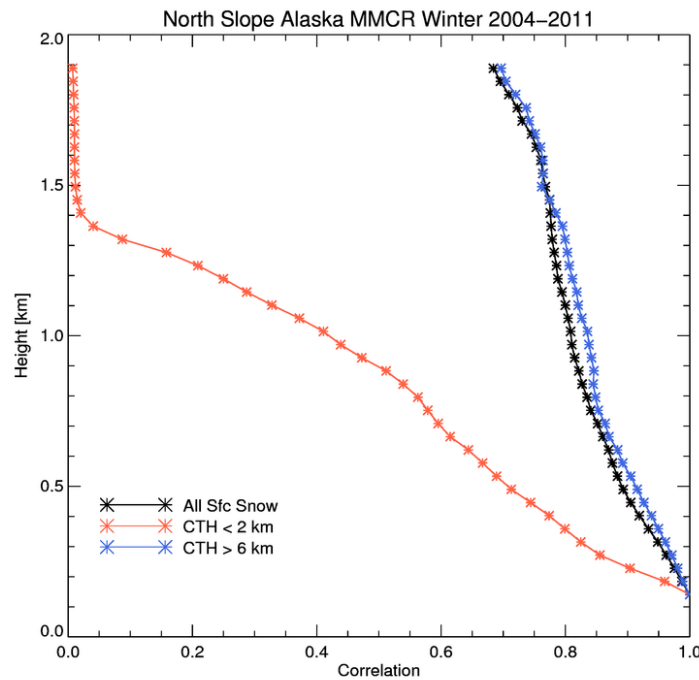
FIGURE 5.13: Correlation of lowest MMCR reflectivity bin to all bins below 2 km for all surface snowfall observations with cloud top heights < 2 km, > 6 km for the entire dataset

Correlations like this allow the near-surface spaceborne snowfall rate measurement error and potential bias to be investigated further to better understand how accurate estimations of reflectivity are below certain levels of CTH for varying snowfall regimes. By comparing two or more different CTH regimes

for the entire dataset, one can gain a better idea of whether or not reflectivity changes appreciably below the usable spaceborne radar bin for each regime. More specifically for this figure, which features the three regimes of the entire dataset (black), CTH's above 6 km (blue) and CTH's below 2 km, the comparison between a shallow regime and a deep regime can be made. The correlation between the reflectivity at the lowest MMCR bin, which is about 125 m, and the bins above 500 m for cases where the CTH's were below 2 km is very low. The correlation is about 0.75 at 500 m, about 0.4 at one km and less than 0.05 above 1.5 km. In comparison, there is a very high correlation between the reflectivity at the lowest MMCR bin and all of the bins above it, up to 2 km for cases where CTH's were above 6 km. For this particular case, the correlation is about 0.9 at 500 meters, 0.8 at 1 km, and about 0.75 for heights above 1.5 km.

The easiest way to visualize the reflectivity correlations on Figure 5.13 is to visualize an imaginary line at the 2 km mark on the earlier daily reflectivities figures, as shown in Figure 5.14. If one were to make a point at 125 meters, note the corresponding reflectivity value and compare to the reflectivity value at a point at 2 km directly above the previous point. If the two reflectivity values are similar there is a higher correlation between the two and vice versa for values that are different.
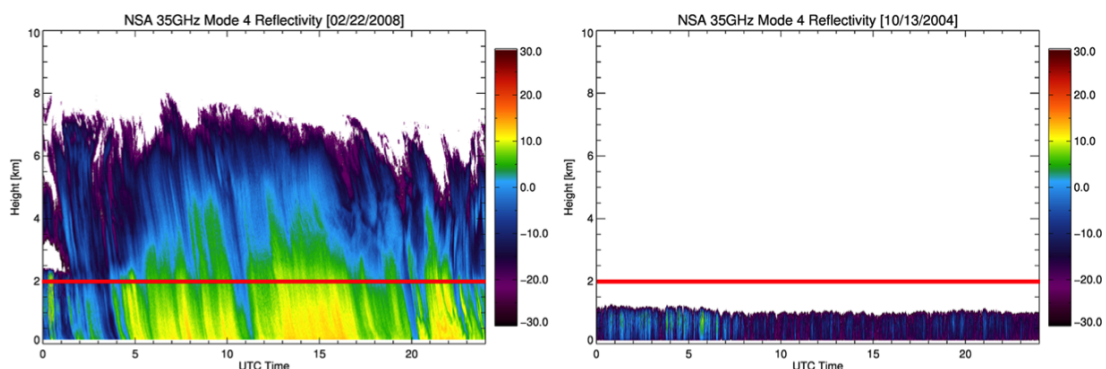
FIGURE 5.14: Daily reflectivity from NSA 35GHz radar with UTC time and height [km] for October 13 2004 and February 22 2008 with a line denoting 2 km in height

Using this method for Figure 5.14 and estimating the correlations between both days shows how different the two reflectivities at each level are for each day. As described earlier, the profile on the left from October, 2004 is a very shallow case, with most CTH's around 1 km, whereas the profile on the right from February, 2008 is a much deeper case with most CTH's above 6 km. These two profiles fulfill each category of previous correlations figure studying cases with CTH's less than 2 km and cases with CTH's greater than 6 km, so the visual comparison of correlation can be easily made. Results from this method clearly show how different the correlations are between these two profiles. For the very shallow case on the left, there is no reflectivity coming close to reaching the 2 km mark, meaning that measurements from a spaceborne product would likely underestimate the reflectivities at the surface. In the deeper case on the right, reflectivities near the surface are very similar to those at the 2 km mark, thus having a high correlation between the two points, which is the opposite of what was seen in the shallow profile. These results further stresses the point of decreasing the blindzone as much as possible, because days where the CTH's remain shallow throughout the day are much more prominent than cases where towering CTH's occur.

To increase the depth of the study into various reflectivity correlations, Figure 5.15 describes the same correlations, however with added CTH thresholds to examine threshold correlation differences as well as to gain a better sense of the overall trend. The additional CTH thresholds are cases where CTH's are less than 1 km, 1.5 km, and 4 km. The overall trend shows that as CTH levels decrease, correlations decrease and vice versa. Once again, at the threshold where CTH's are greater than 6 km there are very high reflectivity correlations. As one moves to the next threshold, CTH's less than 4 km, the reflectivity correlations are much lower with correlation values of 0.7 at 1 km and about 0.4 at 2 km. The less than 2 and 1.5 km thresholds are fairly similar with correlation values of 0.45 at 1km and decreasing at a higher rate past that point. CTH's that are less 1 km show very low correlations. At 500 meters, the correlation value is at about 0.5 and decreases nearly at the same rate after to its
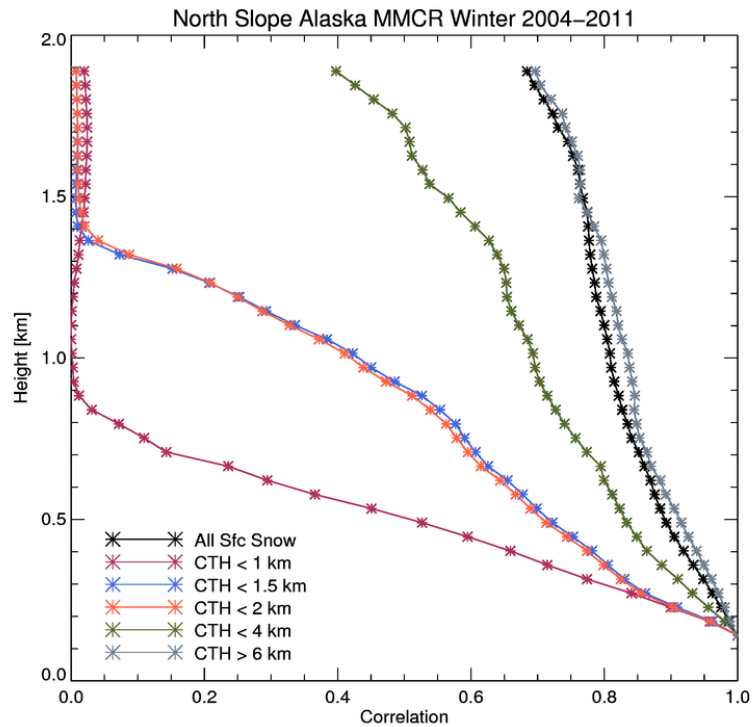
FIGURE 5.15: Same as Figure 5.13, but with added snowfall cloud
top height thresholds of < 1 km, < 1.5 km, and < 4 km

limit of 1 km. Overall, sub-1 km MMCR reflectivity profiles suggest systematic reflectivity increases and snow particle growth, thus spaceborne snowfall rate estimates, and once again, snowfall accumulation may be systematically low at the NSA site and other regions that experience similar snowfall regimes on a regular basis.

One way to further assess these correlation figures is to compare to the mean reflectivity for various cloud top height thresholds to gather a quantitative bias estimate. Figure 5.16 shows the mean reflectivity at all levels and can describe the mean reflectivity at all CTH levels of the dataset. From the surface to just less than 1km, the mean reflectivity is about 1 dBZ but as the height levels increase, the mean reflectivity decreases until reaching the edge threshold of -30 dBZ at just over 7.5 km. The mean reflectivity is about -3, -10, and -20 dBZ at 2 km, 4 km, and 6 km respectively. The decrease in mean reflectivity
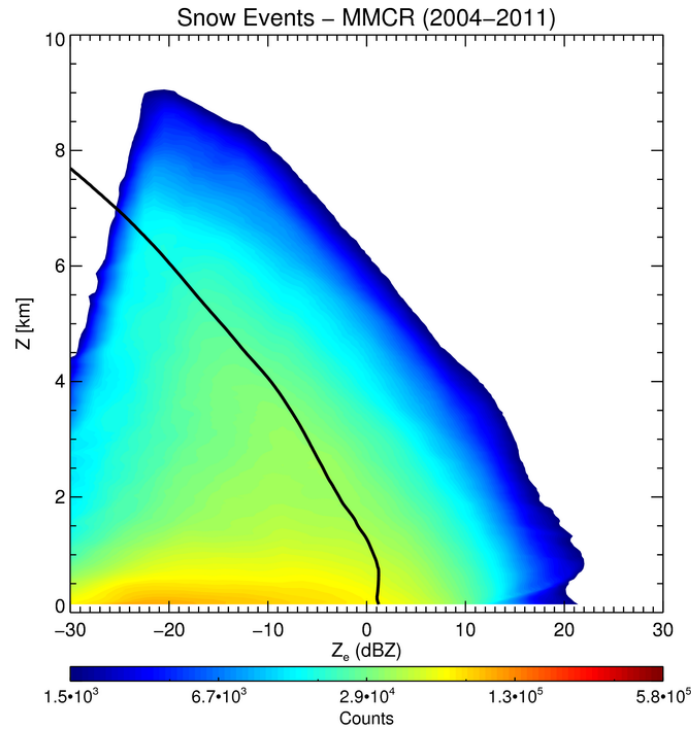
FIGURE 5.16: CFAD displaying the total number of snowfall observations for MMCR reflectivity versus cloud top height for the entire dataset from 2004 to 2011 with a line denoting the mean reflectivity value at each height level
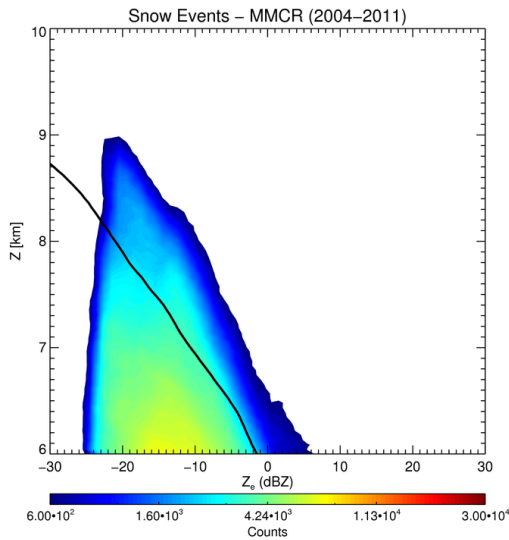
FIGURE 5.17: CFAD displaying the total number of snowfall observations for MMCR reflectivity versus cloud top height for the entire dataset from 2004 to 2011 above 6 km with a line denoting the mean reflectivity value at each height level
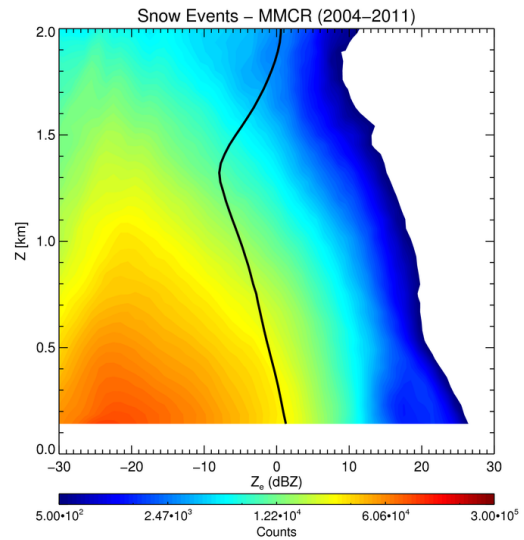
FIGURE 5.18: CFAD displaying the total number of snowfall observations for MMCR reflectivity versus cloud top height for the entire dataset from 2004 to 2011 below 2 km with a line denoting the mean reflectivity value at each height level

with height is large, especially for events above 1 km in CTH. This analysis is noteworthy in that it delivers insight into what future spaceborne radars need to be capable of when determining what near-surface height (lowest bin) would be appropriate for the most cost-effective and accurate measurements possible.

To gain another perspective using this approach, mean reflectivities were taken for certain CTH thresholds. Figure 5.17 describes deeper snowfall events of greater than 6 km, and Figure 5.18 describes shallow snowfall events less than 2 km. This offers slightly different results and allows for the investigation into potential spaceborne radar biases, especially when analyzing the shallow CTH threshold. For the results of the greater than 6 km threshold, the mean reflectivity at 6 km is about -1 dBZ and decreases with height. This result reiterates the sharp decline in mean reflectivity as height increases as seen on the previous figure. Moving to the shallow threshold of less than 2 km, the mean reflectivity at the surface is about 2 dBZ and decreases with height until about 1.35 km at about -9 dBZ, where an inversion occurs and the mean reflectivity increases to just over 0 dBZ at 2 km. The most applicable point this figure shows is the potential spaceborne radar bias in the blindzone below 1 km. The mean reflectivity at 1 km is about -5 dBZ, meaning there is a negative bias of over 6 dBZ, if it is assumed the mean reflectivity continues to increase even below the lowest radar bin toward the surface. This means that spaceborne radar platforms with a lowest detectable radar bin of 1 km potentially underestimate reflectivity at the surface by 6+ dBZ at Barrow, AK, which can have a large effect on a variety of factors including snowfall rates and accumulation totals at the surface. Using these for future radar platforms can act as a way to analyze the potential radar bias if that lowest detectable radar bin was lowered further. For example, if a future spaceborne radar platform had a lowest detectable radar bin of 500 m, the mean reflectivity is about -1 dBZ, meaning there is a negative bias of about 2+ dBZ, which is a strong improvement from a 1 km radar bin. This analysis is very valuable to consider for current and future spaceborne radar platforms.

5.3 Investigation of Spaceborne Radar Bias – Section Summary

• Reflectivity correlations at levels below 4 km are very low and decrease with decreasing height levels, whereas cloud levels above 6 km show very high correlations below 2 km.

• Mean reflectivity at the surface is about 1 dBZ decreases with height to -30 dBZ at about 7.5 km for the total dataset.

• Observations below 2 km show a negative radar bias of just over 6 dBZ when measuring at a blindzone level of 1 km to the surface. This decreases to just over 2 dBZ if the blindzone level were decreased to 500 m.

5.4 Snowfall and Associated Environmental Parameters

- Cloud Top Height, Wind Speed/Direction, Barometric Pressure, Temperature, Relative Humidity, Snowfall Rate

The next step in this research project is to investigate the many environmental parameters the surface MET provides in order to gain a better sense of what environmental conditions, if any, control certain snowfall regimes at the NSA site. This information from the MMCR can be very useful for the configuration of future spaceborne radars, since they can be optimally tuned to study the snowfall regimes controlled by certain parameters. The first phase of this analysis is the study of the overall frequency of occurrence of very shallow cases where CTH is below 1 km (Figure 5.19). Figure 5.19a describes the occurrences of reflectivity for all cases of CTH less than 1 km for the entire seven year dataset, while Figure 5.19b describes each individual year of the dataset to show the variability in the overall trend. From this figure, the general strength, in terms of reflectivity, can be determined for very shallow snowfall cases. Shallow cases are of particular interest as well since shallow
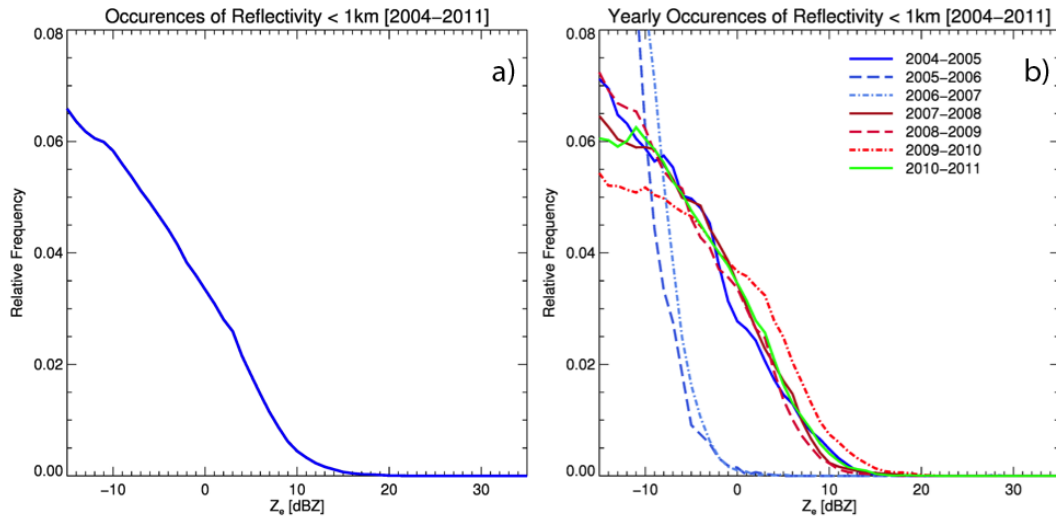
FIGURE 5.19: Relative frequency of occurrence of reflectivity for cloud top heights less than 1 km for the entire dataset averaged for the entire dataset (a) along with each individual year of the dataset (b)

snowfall is often forced by wind blowing over ice free warmer waters. Most reflectivity values fall below 15 dBZ, as nearly 0% of all occurrences are above this level for observations below 1 km in CTH. The peak in occurrence of 0.065 at the lowest threshold of -15 dBZ, which was used to tabulate reflectivity distribution figures in order to conform with CloudSat's 2C-SNOW-PROFILE algorithm. On a yearly scale, there is a lot of variability. As shown in the earlier study of yearly variability, some years like 2005-2006 have a higher occurrence of shallow, light snowfall whereas other years like 2009-2010, it's more common to have higher reflectivity values, even given the shallow CTH's.

Increasing the CTH threshold to study the occurrences of reflectivity less than 2 km for the entire dataset, Figures 5.20a and 5.20b shows similar results. A 1 km CTH threshold increase allows two shallow snowfall categories to investigate the potential differences between the two snowfall regimes. Overall, the general trend of a high occurrence of light reflectivities remains the same, however there are some slight differences to note. There is a very slight increase in occurrences for the maximum reflectivity (above 10 dBZ) and the peak in occurrences at just lower than -15 dBZ has slightly decreased
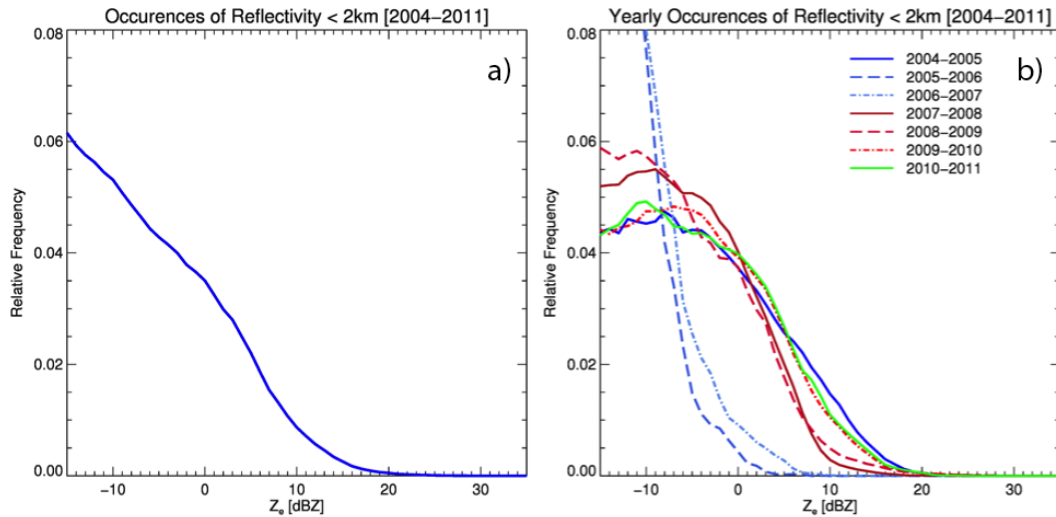
FIGURE 5.20: Same as Figure 5.19, but for cloud top heights less
than 2 km

to about 0.06. This is mainly due to the increase in occurrences above these
two reflectivity levels, respectively. About 0% of snowfall events were greater
than -15 dBZ and less than 1 km, but 0.07% of snowfall events were greater
than -15 dBZ and less than 2 km. Also, the number of snowfall events greater
than 10 dBZ increased from about 0.04% to 0.35% for events above 1 km and 2
km respectively. On a yearly scale, the different values and variability largely
remain the same or are very similar with slight increases in occurrences at
higher reflectivity values. 2005 through 2007 are two years where shallow and
light snowfall events below -5 dBZ were very predominant, while years like
2004-05 and the two years of 2009-11 showed a much higher distribution of
reflectivities above -5 dBZ and even 10 dBZ when compared to the other years
with generally stronger events.

The next environmental parameters to study are wind speed and wind di-
rection and the amount of times snowfall occurs given a certain wind speed
and direction, as shown in Figure 5.21. Due to the location of Barrow, AK
and overall exposure of the NSA site (Figure 2.4), studying which direction
snowfall events occur most often can help to give a better idea of how and
where they snowfall events manifest from and the possible oceanic influence
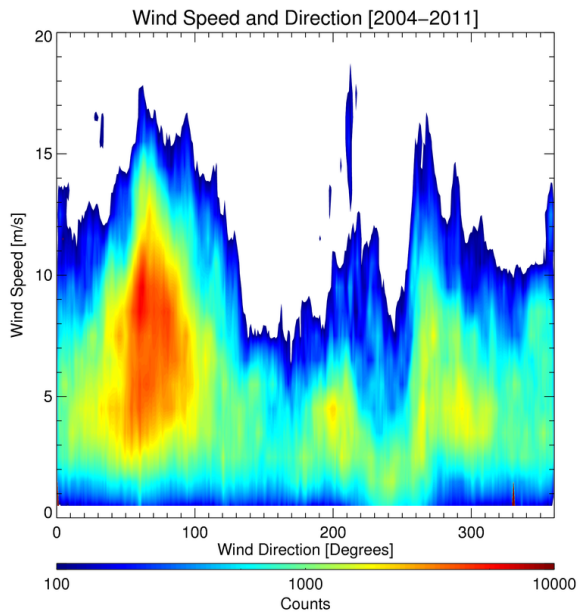
FIGURE 5.21: Total number of snowfall observations for wind direction [Degrees] versus wind speed [ms-1] for the entire dataset
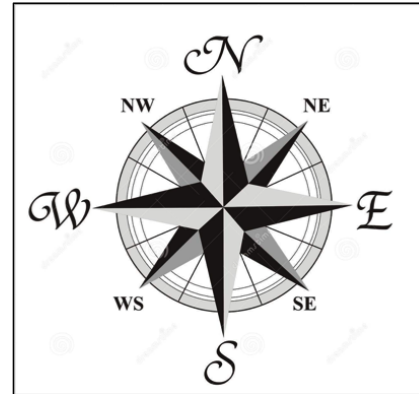
FIGURE 5.22: Wind rose figure describing the cardinal directions in association with Figure 5.21 and the corresponding wind direction

on NSA snowfall. At the NSA site, the highest amount of counts of snowfall events are from between 0° and 90° or the northeastern sector of the windrose in Figure 5.22. Also of note are the relatively high wind speeds, especially in the northeastern sector, of 5-15 m/s, which is likely a result of the aforementioned exposure of Barrow, AK. The wind direction trends remain consistent, specifically in deeper cases as well, which aren't shown.

To further study wind direction, the next logical step is to investigate the relative strength, based on MMCR lowest bin reflectivity, of the snowfall events for quadrant of the windrose, in order to see whether or not there is a certain direction where the strongest snowfall events occur. Figure 5.23 describes the relative frequency of occurrence of reflectivity for each year of data, for each quadrant. Observing all four quadrants for the entire dataset shows no clear trend as far as relative strength of the snowfall events for each direction. On a yearly scale, there are some inter-annual trends. For example, in 2004-2005, the two eastern quadrants (Figures 30a and 30b) show peaks of occurrences at around 5 dBZ, whereas, the two western quadrants (Figures 5.23c and 5.23d) show peaks of occurrences at about -5 to -10 dBZ showing that snowfall events
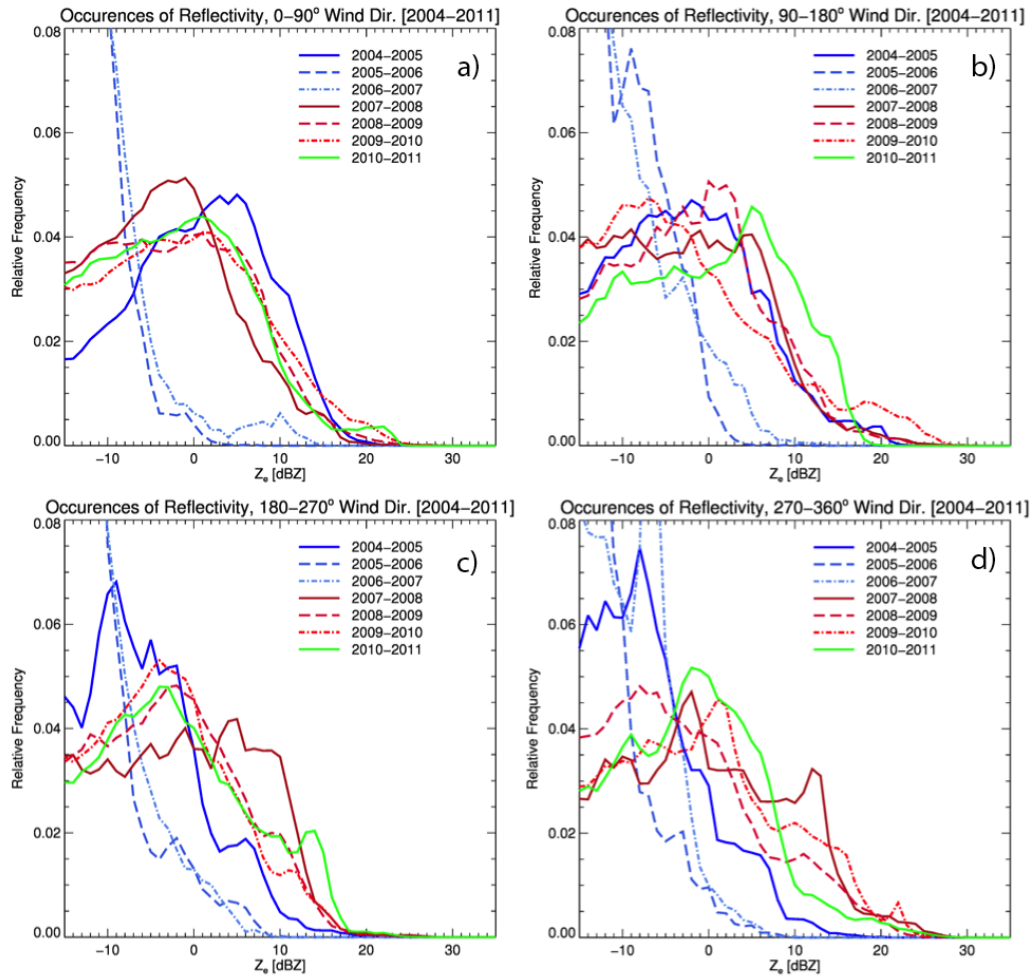
FIGURE 5.23: Relative frequency of occurrence of reflectivity for wind direction from 0°-90° (a), 90°-180° (b), 180°-270°(c), and 270°-360° (d), respectively, for each individual year of the dataset

were relatively stronger when snowfall events had a wind direction from the east than when they had a wind direction from the west. This trend, however, isn't consistent throughout the entire dataset as most years tend to stay very similar throughout all four quadrants or there is a year like 2007-2008, where there isn't a clear trend. In 2007-2008, for the northeastern quadrant, the peak of frequency of occurrence is around 0 dBZ, but the two southern quadrants are at a consistent level of just less than 0.04 in relative frequency. The northwestern quadrant meanwhile has a peak in relative frequency at around -2 dBZ and decreases with higher reflectivity until about 13 dBZ, where there is a second peak in relative frequency before decreasing again. Overall, there is no easily

observable trend of the relative strength of the snowfall events that occur in a certain wind direction at NSA.
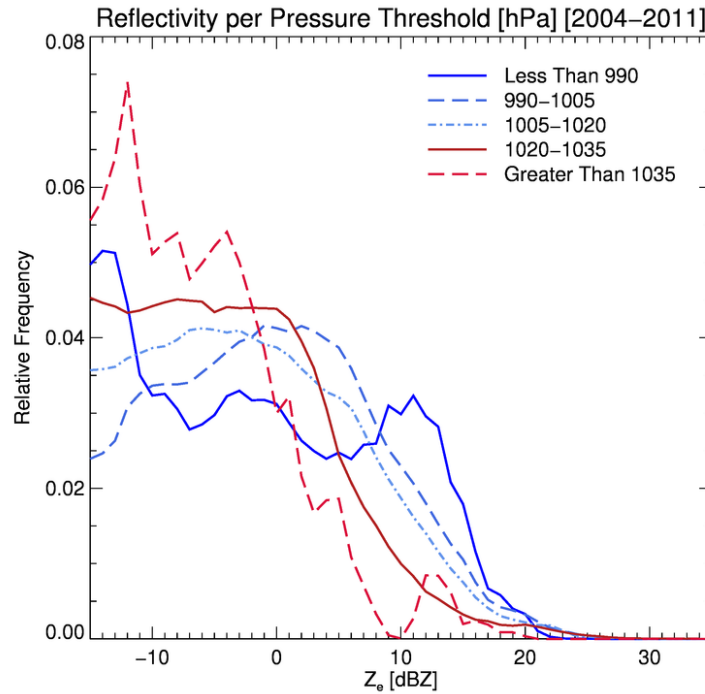
FIGURE 5.24: Relative frequency of occurrence of reflectivity for multiple thresholds of barometric pressure [hPa] for the entire dataset

Another environmental parameter to consider is the barometric pressure in hectopascals (hPa). From Figure 5.24, which shows the relative frequency of occurrence of reflectivity for given pressure threshold (less than 990 hPa, 990-1005 hPa, 1005-1020 hPa, 1020-1035 hPa, and greater than 1035 hPa), a view of what type of pressure systems correspond to what kind of snowfall events can be observed. This analysis attempts to answer whether the total accumulation of snow is mainly bolstered by the very rare, very strong snowfall events associated with deep low pressure systems or if the total accumulation is mainly comprised mostly of shallow, light snowfall cases. In general, the trend is that lower pressure corresponds to higher reflectivity and vice versa. By partitioning the minimum and maximum thresholds and observing individually, it is easy to note the differences between the two surface pressure

and snowfall intensity paradigms. The minimum pressure threshold of less than 990 hPa shows a peak in frequency of occurrence of 0.03 at just above 10 dBZ, which is well above any other threshold and the maximum pressure threshold of greater than 1035 hPa shows a peak in frequency of occurrence of 0.075 at just below -10 dBZ, which above the other thresholds as well.
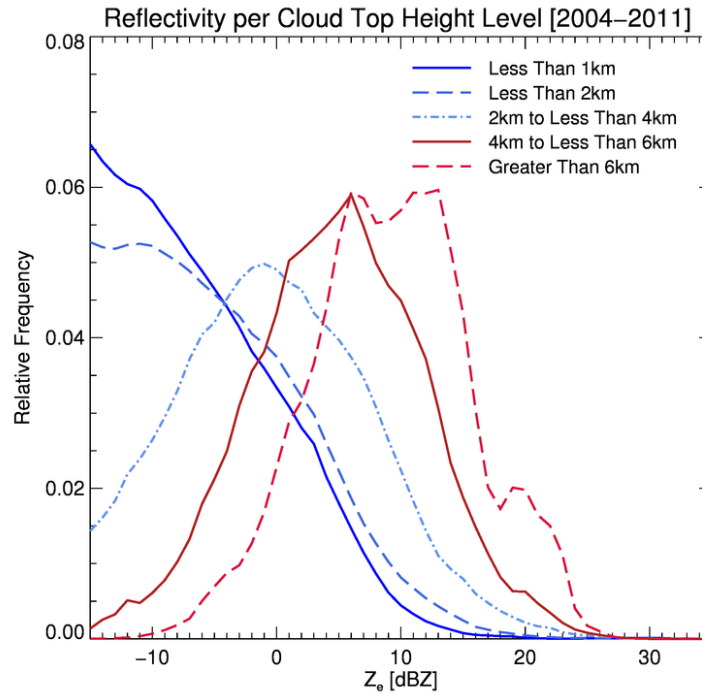
FIGURE 5.25: Same as Figure 5.24, but for multiple thresholds of cloud top height [km]}

In a similar experiment to above, the relative frequency of occurrence of reflectivity at various CTH thresholds for the entire dataset was examined, as shown in Figure 5.25. The CTH thresholds are less than 1 km, less than 2 km, two to 4 km, 4 to 6 km and greater than 6 km. This type of study helps explore whether or not there is a similar trend as the pressure study above and if there are any vast differences between any of thresholds that might further separate the numerous snowfall regimes. Overall, there is a clear trend showing that the higher the CTH, the higher the reflectivity and vice versa. This corresponds with the previous pressure threshold figure, as lower pressure systems are

more likely to bring deeper snowfall events and higher pressure systems are more likely to bring shallower snowfall events. The two minimum thresholds of less than 1 and 2 km were described earlier, but in comparison to the other thresholds, show a much higher relative frequency of occurrence at very light reflectivities. Above these two levels, the peaks of occurrences fall between 0-15 dBZ, demonstrating that, in general, snowfall events with CTH's above 2 km are much stronger in comparison.
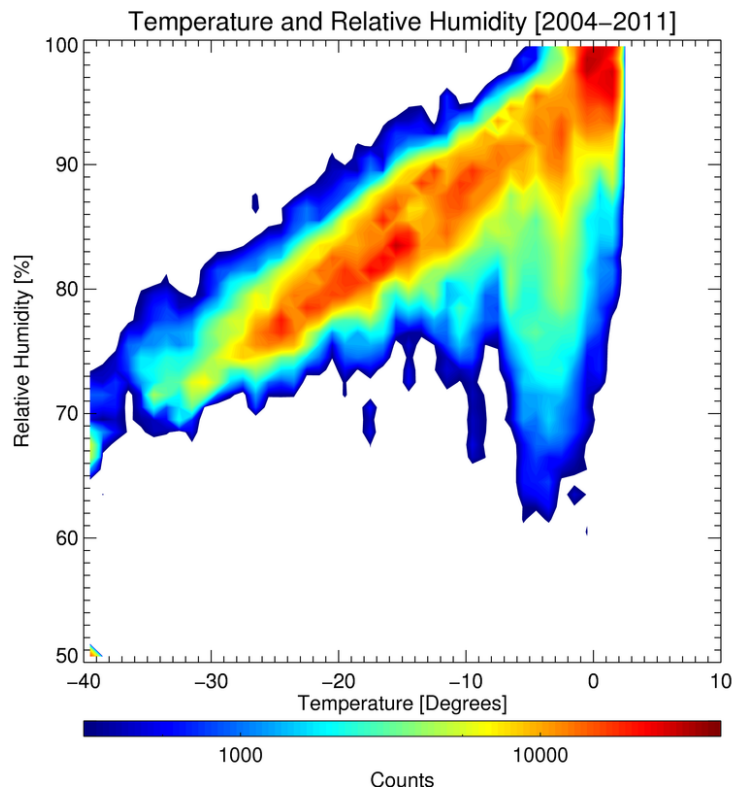
FIGURE 5.26: Total number of snowfall observations for temperature [°C] versus relative humidity [%] for the entire dataset

Temperature and relative humidity (with respect to water) are another set of environmental parameters to study, which is shown in Figure 5.26. The combination of the two serve as a way to further investigate snowfall's dependency on various parameters to have a better idea of what are the main factors that contributes to snowfall events. At the NSA site, there is almost a positive linear trend toward higher temperatures and higher relative humidities. This trend starts from about 70% relative humidity and -35°C and continues up until the

limit of 100% relative humidity and 2°C. In between -10° and 0° the pattern of observed counts strays from the trend line and shows that in this temperature range, snowfall events can occur at any relative humidity value above 60-65%. The temperature range with the highest amount of counts is between 0 to -5°C where 22% of the total counts fall into this threshold. The next highest range is a tie between -5 to -10°C, -10 to -15°C, and -15 to -20°C, which all account for about 15% of the total counts, respectively. On the relative humidity side, about 46% of the total counts occur in the range between 80 to 90%. These characteristics remain consistent throughout all cloud top height levels as well.
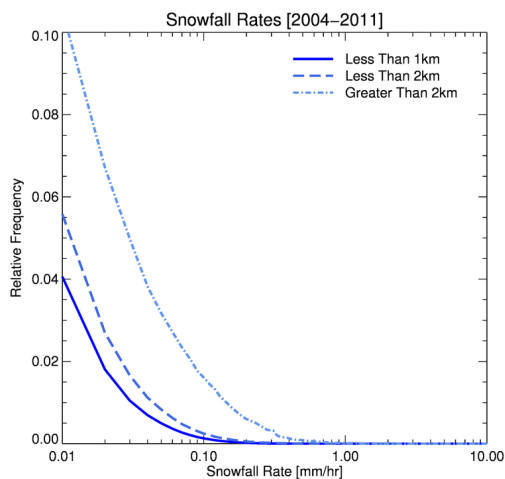
FIGURE 5.27: Relative frequency of occurrence of reflectivity for snowfall rate [mm hr-1] for multiple thresholds of cloud top height [km] for the entire dataset
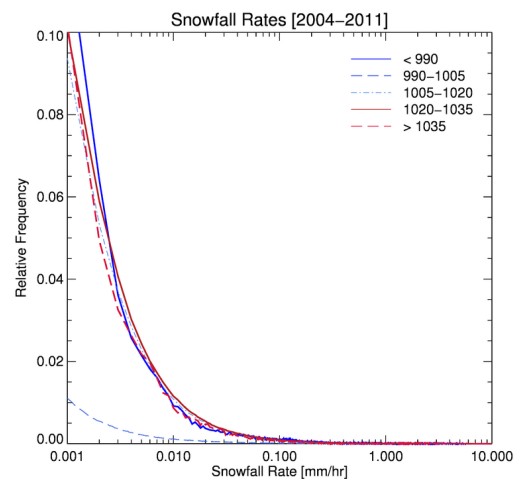
FIGURE 5.28: Same as Figure 5.27, but for multiple thresholds of barometric pressure [hPa]

The investigation of snowfall rates is another aspect of interest. Figure 5.27 describes the relative frequency of occurrence of the calculated snowfall rates at certain CTH thresholds. The study of snowfall rates is once again another piece to the answer to define the overall scene of accumulation at the NSA site. By identifying the snowfall rates at certain CTH's, it can be observed how different very shallow snowfall cases are to deeper snowfall cases when it comes to snowfall rates. According to this figure, the overall relative frequency of snowfall rates increases in all rates shown and also show an increase in

snowfall rates (above 0.1 mm/hr) when the CTH is greater than 2 km. For the shallow cases of less than 1 km and less than 2 km, there is a slight increase in overall frequency with an increase in CTH of occurrence but the maximum snowfall rate is just over 0.1 mm/hr. In conclusion, the higher the CTH the larger the snowfall rate, which corresponds to the earlier analysis where about 18% of total accumulation counts were below 2km in cloud top height, whereas nearly 22% of total accumulation counts were above 6km.

Much like the earlier figures describing the reflectivity based on thresholds and CTH and pressure and comparing the two, the same can be done for snowfall rates, as shown in Figure 5.28. The main reason to study pressure thresholds and their corresponding snowfall rates is to receive an indication of whether or not low-pressure systems would bring much larger snowfall rates as opposed to high-pressure systems at Barrow, AK. The results show that in general snowfall rates increase with lower pressure, which was expected based on the previous results. Once again, partitioning the minimum (less than 990 hPa) and maximum (greater than 1035 hPa) thresholds of pressure shows a pretty large difference in the relative frequency of occurrence for snowfall rates. For the maximum threshold, almost all cases observed were below 0.1 mm/hr, whereas many more occurrences in the minimum threshold were above 0.1 mm/hr. In total, snowfall rates increase with lower pressure systems and greater CTH's.

5.4 Snowfall and Associated Environmental Parameters – Section Summary

- Yearly variability exists throughout most environmental parameters.

- Most wind direction counts are from the northeast wind direction, but no observable trend exists in terms of relative strength of snowfall events using reflectivity.

- The relative frequency of occurrence at higher reflectivity increases with lower pressure/higher CTH's and vice versa for higher pressure/lower CTH's.

- Positive trend for temperature and relative humidity with snowfall events, with most counts occurring at higher temperature (above -10°C).

- The relative frequency of occurrence at larger snowfall rates increases with lower pressure/higher CTH's and vice versa for higher pressure/lower CTH's.

5.5 Investigation of Ice Coverage Impacts

- Associated Environmental Parameters: Cloud Top Height, Barometric Pressure, Temperature, Relative Humidity, Wind Direction, and Snowfall Rate

The last area of interest consists of utilizing the NSIDC data, which provides valuable ice coverage over the ocean data that can be used to further partition the dataset into cases where there is ice/no ice coverage over the surrounding ocean just off the coast of Barrow, AK. Figure 5.29 offers a simple comparison of relative strength of snowfall cases using reflectivity between cases where there is ice coverage and cases where there is open ocean. As a reminder, these ad hoc thresholds were determined as any observation with an ice fraction at or above 90% would be considered ice covered and any observation with an ice fraction at or below 10% would be considered open ocean. When dividing the dataset in this way, there are just over 3.16 million ice covered counts and about 330,000 open ocean counts. This accounts for 76% and 8% of the entire dataset. Each case show a very similar trend where the relative frequency of occurrence is mostly the same until about 5 dBZ where it falls off drastically as reflectivity exceeds 20 dBZ and beyond. Some slight differences exist however, as the relative frequency of occurrence for open ocean cases is slightly lower for lower reflectivities and vice versa for higher reflectivities in comparison to ice covered cases. Another area of difference is in the range around 10 dBZ where there is a higher relative frequency of occurrence for open ocean cases

that is notably higher than the same reflectivity region for ice covered cases. The two cases, as a whole, are very similar however some differences exist and could be further shown if the dataset is divided up using the environmental parameters that were discussed in the previous section.
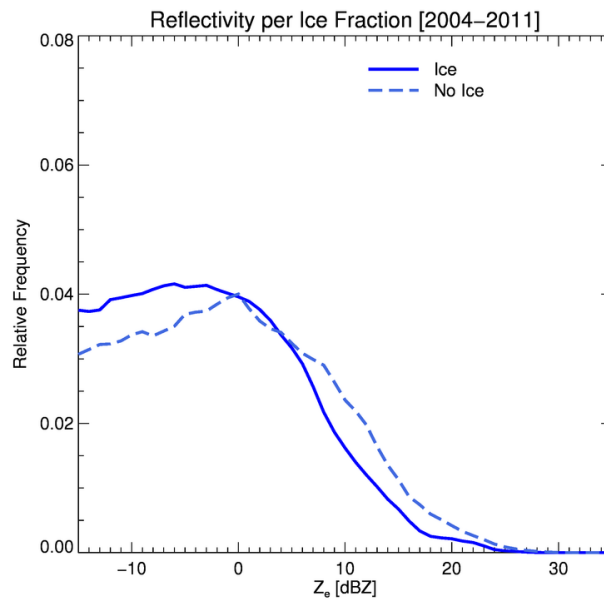
FIGURE 5.29: Relative frequency of occurrence of reflectivity for ice covered and open ocean cases for the entire dataset
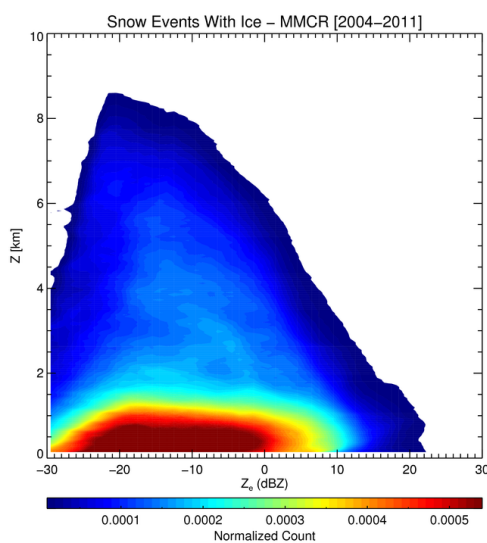
FIGURE 5.30: CFAD displaying normalized snowfall observations for ice covered cases for the entire dataset
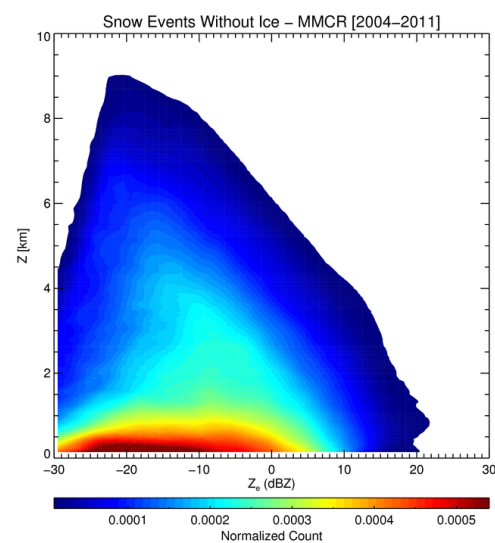
FIGURE 5.31: Same as Figure 5.30, but for open ocean cases

In order to further assess the two cases, two normalized CFADS, as shown in Figures 5.30 and 5.31 can give a better idea of where MMCR reflectivity structural differences between the two ice-related snowfall regimes. One notable difference that exists between the two cases, is that in the reflectivity range of -25 and 0 dBZ, there is a greater concentration of normalized counts for cases with an ice covered ocean at shallow CTH's, specifically below 1 km. In roughly that same range however, there are higher normalized counts above 1 km, but below 4 km, indicating that snowfall events with reflectivities around -10 dBZ are generally deeper snowfall events. From these figures, it can be gathered that very shallow snowfall events are stronger in terms of reflectivity compared to open ocean cases, but that open ocean oceans are more prone to deeper CTH events for middle to light reflectivities.
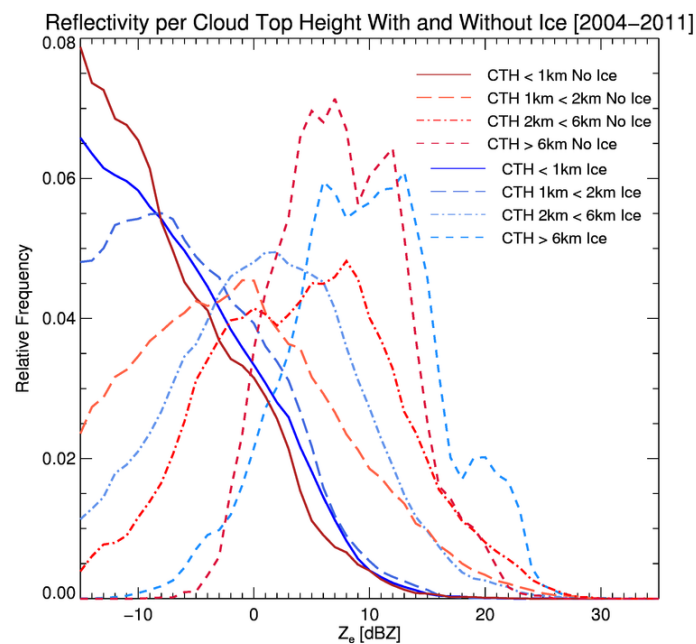
FIGURE 5.32: Relative frequency of occurrence of reflectivity for cloud top height thresholds of less than 1 km, 1 to 2 km, 2 to 6 km, and greater than 6 km for both ice covered and open ocean cases for the entire dataset

CTH thresholds are first used to partition this dataset in order to observe if there are clear differences between CTH regimes as shown in Figure 5.32. There

are many similar trends for each threshold, but magnifying the two cases for every CTH regime can show differences between the two cases. Starting with the lowest CTH threshold of less than 1 km, which includes all snowfall observations with a CTH below 1km, the overall trend is the same as the relative frequency of occurrences peak at the edge threshold of -15 dBZ and decrease as the reflectivities get higher. The peak in relative frequency of occurrence is higher by 0.015 for open ocean cases, however at higher reflectivities, most notably the range from -5 dBZ to 10 dBZ, the relative frequency of occurrence is actually higher for ice covered ocean. Moving up to cases between 1 km and 2 km in CTH, which includes all observations with a CTH above 1 km but below 2 km, there is a relatively similar trend. The relative frequency of occurrence peak is at -10 to -5 dBZ (0.05) and 0 dBZ (0.045) for ice covered and open ocean cases respectively, and they each decrease in relative frequency with higher reflectivities. The differences for the two cases are clear, as open ocean cases are generally stronger in terms of reflectivity for this threshold. The results are actually flipped from the previous threshold, as open ocean cases show slightly higher relative frequency of occurrences at higher reflectivities.

Continuing to the next threshold of cases between 2 km and 6 km, which covers most of the observations, shows a similar trend to the previous threshold. The maximum relative frequency of occurrences (0.05) stretches from about -5 dBZ to about 5 dBZ for ice-covered cases and then proceeds to decrease as reflectivities increase. For open ocean cases, the peak in relative frequency of occurrence is at about 10 dBZ with a value of about 0.05. The most notable difference between the two cases is that the open ocean case has higher relative frequency of occurrences for higher reflectivities, similar to the previous threshold. The last threshold for cases above 6 km in CTH, show the greatest variability. The peak in relative frequency of occurrence is at about 5 to 15 dBZ and varies largely as cases without ice have a peak relative frequency value of 0.07 and cases with ice have a peak relative frequency value of about 0.06. Cases with ice also show a higher relative frequency of occurrence for reflectivities above 15 dBZ and vice versa for reflectivities below 5 dBZ, signaling cases that meet

these criteria are stronger as compared to its counterpart. An overall trend seen with each threshold is that the relative frequency peak continually shifts to higher reflectivities with higher CTH thresholds, which remains consistent with earlier CTH threshold with reflectivity figures. An interesting aspect is how open ocean cases at the edge CTH thresholds (<1km, >6km) show higher relative frequency values at higher reflectivities, whereas this trend is flipped for the middle two CTH thresholds.
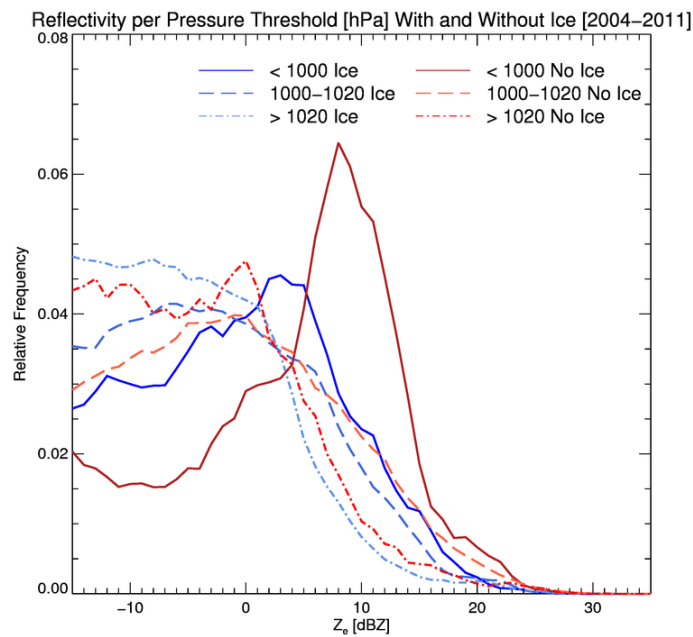
FIGURE 5.33: Same as Figure 5.32 but for the pressure thresholds of < 1000 hPa, 1000-1020 hPa, and > 1020 hPa

Another way to partition the data in a similar fashion to CTH is by utilizing multiple barometric pressure thresholds for each case, which is shown in Figure 5.33. Using various pressure thresholds and comparing each case will show whether or not low or high-pressure systems have different effects for each ice coverage case. Comparing the highest pressure threshold of greater than 1020 hPa shows a very similar trend between the two cases. For the most part, not much separates the two cases in terms of relative frequency of occurrence throughout all of the reflectivities. The most notable difference occurs between

-15 and 5 dBZ where the relative frequency of occurrence is slightly lower in cases with an open ocean for each respective threshold. The middle threshold of 1000-1020 hPa shows a very similar trend throughout as well. There are only slight differences in relative frequency of occurrence throughout most of the reflectivity spectrum. Open ocean cases show lower/higher relative frequency of occurrences when the reflectivity is between -15 and -5 dBZ/5 and 25 dBZ when compared to their counterpart threshold with ice-covered ocean cases.

The range that shows the largest differences is cases below 1000 hPa. Cases without ice have lower relative frequency of occurrences for most reflectivity values, however in the range between 5 and 15 dBZ, there is a very large peak in relative frequency of occurrence. This cause of this is unknown, but it may be due to the smaller sample size of observations in this threshold for open ocean cases. There are only about 29,000 observations in this threshold, which contributes to only 0.7% of the total observations for both cases and 8.6% of total observations for open ocean cases, which is much lower than the other two thresholds. Overall, these two cases do not show many discernible differences until low-pressure systems differentiate the two categories.
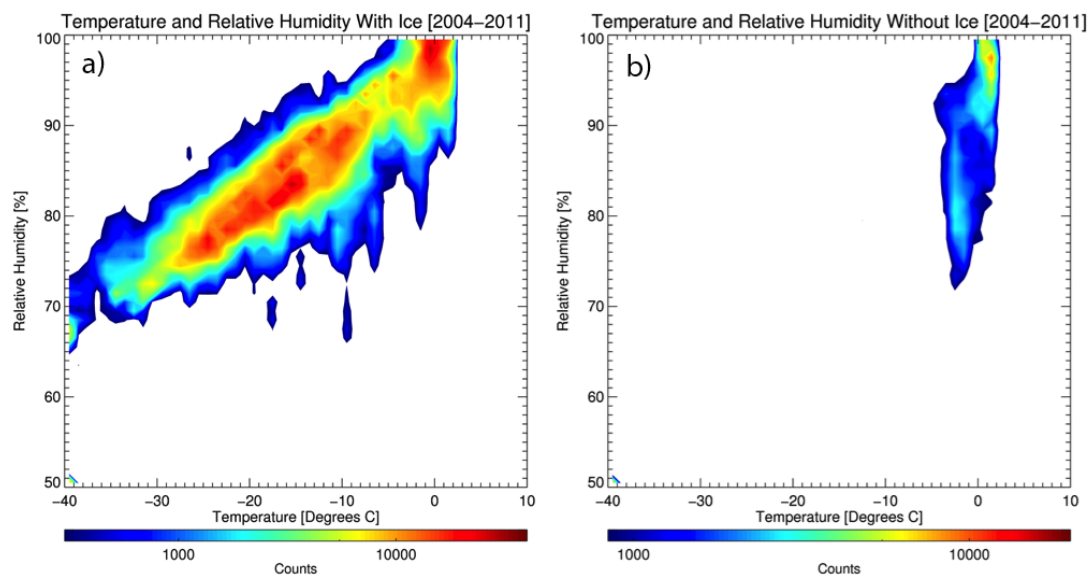
FIGURE 5.34: Total number of snowfall observations for temperature (°C) versus relative humidity (%) for the entire dataset for ice covered cases (a) and open ocean cases (b)

Two more parameters of interest include temperature and relative humidity of each case. This comparison is shown in Figure 5.34 and is useful because it can show snowfall dependence on certain relative humidity and temperature patterns for open ocean and ice covered situations. Figure 5.34a shows the total number of snowfall observation given certain temperature and relative humidity values for cases with an ice covered ocean and Figure 5.34b is the same but shows open ocean cases. Overall, the real striking difference between the two cases is the temperature at which snowfall occurs. The observations for an ice-covered ocean are evenly distributed among the temperatures shown and follow a positive linear trend with relative humidity. As expected, open ocean snowfall events are associated with higher temperatures in the fall and early winter seasons. Most open ocean snow events are above -5°C. An interesting aspect is the relatively even distribution of observations for relative humidity above 70% and there is no linear trend as seen in the cases with an ice-covered ocean. In comparison with Figure 33, which shows all of the counts, the two cases reveal the causes between the different regions on the figure, particularly the positive trend line with many counts, and the feature from -5-2°C with numerous counts at varying relative humidities. This provides added explanation about what environmental factors contribute to various snowfall regimes in this region.

Incorporating wind direction as the next parameter is another necessary step when examining these two cases. Figure 5.35 shows the relative strength based on reflectivity for both cases of ice coverage. In Figure 5.35a, cases with ice coverage are split into the four quadrants of the wind rose, as shown earlier with Figure 5.22, and the same is shown in Figure 5.35b, however for cases with open ocean. This type of analysis allows for the determination of whether or not wind direction correlates to certain trends like relative strength of snowfall events. For cases with ice coverage, no direction clearly differentiates itself from the other as they all have the same trend of remaining roughly constant at a relative frequency of about 0.04 until decreasing to nearly zero starting at about 0 dBZ. Small differences include a pattern of higher relative frequency of
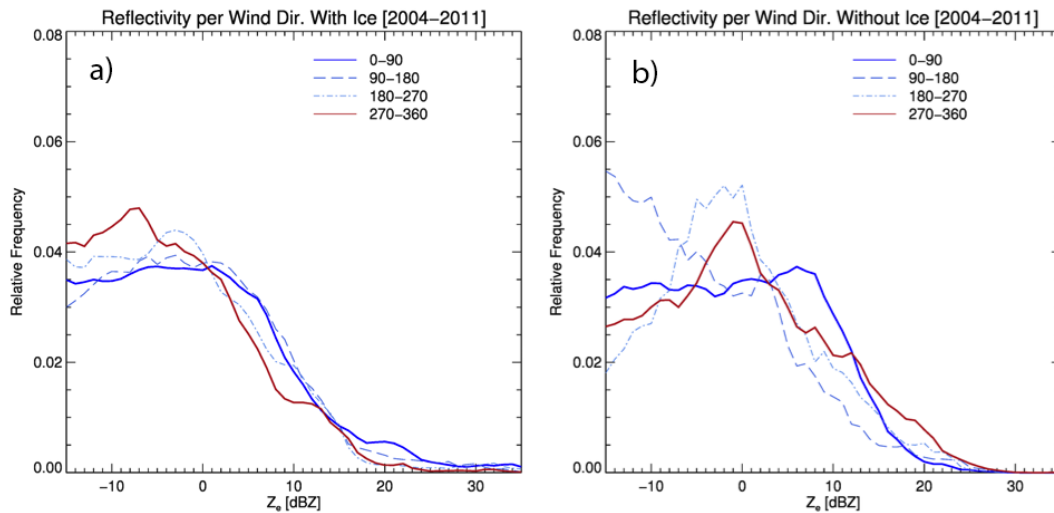
FIGURE 5.35: Relative frequency of occurrence of reflectivity for
wind direction from 0°-90°, 90°-180°, 180°-270°, and 270°-360° for
ice covered (a) and open ocean cases (b) for the entire dataset

occurrences in lower reflectivities and vice versa for higher reflectivity for the
270°-360° wind direction and a slight peak in relative frequency of occurrence
just less than 0 dBZ for the 180°-270° wind direction.

Cases with an open ocean showed more differences. The northern two quadrants (270°-90°) were very similar with the only large difference being their
peak in relative frequency of occurrence, which is about 0.035 at 5-10 dBZ for
0°-90° and 0.045 at 0 dBZ for 270°-360°. The southern two quadrants were
unique in comparison. The 90°-180° wind direction has much higher relative
frequency of occurrences for lower reflectivities and vice versa for higher
reflectivities and the 180°-270° wind direction shows an extensive peak in
relative frequency of occurrence of 0.05 around 0 dBZ. When comparing both
partitioned cases directly, as shown in Figure 5.36, The two southern quadrants
from the open ocean cases really stand out, especially considering the other six
partitions for each case show roughly the same trend.

Using the wind direction environmental parameter to partition each case
yields an interest into analyzing whether or not these characteristics vary
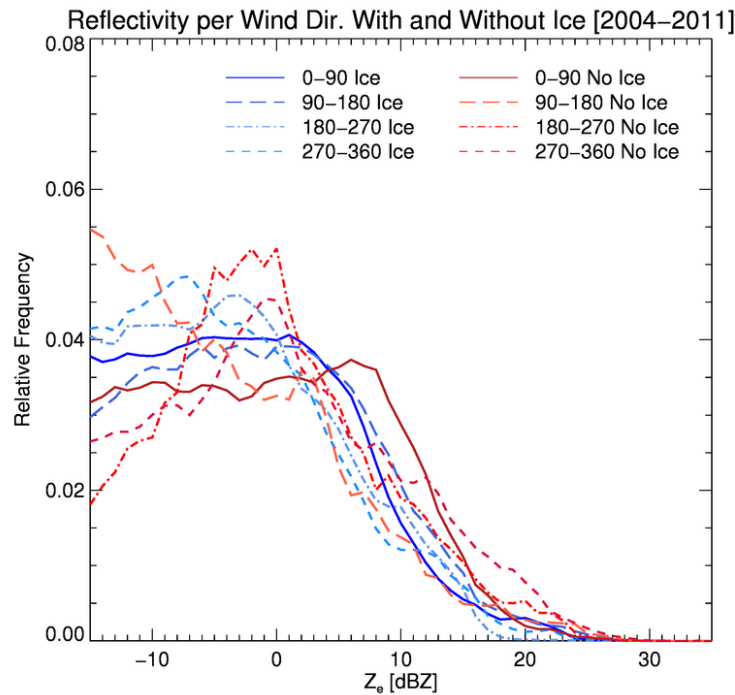
FIGURE 5.36: Same as Figure 5.35, but combined for both cases of ice coverage
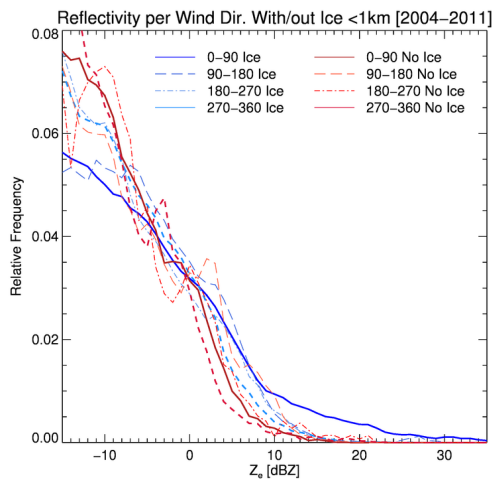
FIGURE 5.37: Same as Figure 5.36, but for events below 1 km in cloud level
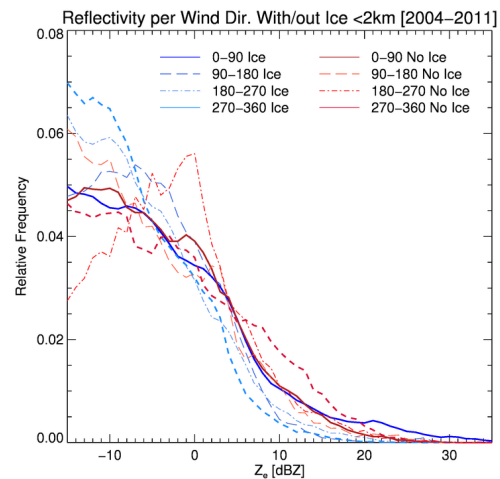
FIGURE 5.38: Same as Figure 5.36, but for events below 1 km in cloud level

when exposed to a CTH threshold for shallow snowfall events. Once again, shallow cases are of particular interest as well since shallow snowfall is often forced by wind blowing over ice free warmer waters, so finding differences between the two cases during shallow snowfall events is valuable. Figure 5.37,

describes snowfall cases below 1 km, partitioned by each case and each wind direction. Overall, there is a similar trend between all situations where the peak in relative frequency of occurrence is at around -15 to -10 dBZ and decreases from that point onward. One difference is that open ocean cases have a higher relative frequency of occurrence in lower reflectivities and vice versa for higher reflectivities meaning that snowfall events that fit this criteria are more likely to be weaker in terms of strength as compared to cases with an ice covered ocean. Snowfall events with CTH below 2 km for the same data partitioning scheme, as shown in Figure 5.38, provides more differences. The majority of partitions follow the same trend of a decreasing relative frequency as reflectivity increases, especially at about 0 dBZ. Each case is variable below that level in reflectivity however as the range in relative frequency values for each case stretches from about 0.03 to 0.07 at -15 dBZ. They eventually even out at come closer to a similar relative frequency value of 0.375 at 0 dBZ. One stand out feature is the 180°-270° wind direction in an open ocean, where there is a large relative frequency peak at about 0 dBZ that is much different than the other cases. This corresponds similarly to what was seen when observing all of the cases without a CTH in Figure 43, where the same partition showed a similar peak in relative frequency of occurrence.

One final way to assess the impact of wind direction for each case is to analyze the normalized counts for each case, for the four different wind directions as shown in Figures 5.39 and 5.40. Starting with the ice covered case (Figure 5.39), which describes the CTH and reflectivity setting for ice covered cases in each wind direction, the four wind directions are generally similar, however, slight differences occur, especially at or below 2 km in height. The majority of normalized counts are below 2 km 0 dBZ for all wind directions. One small trend is that there are higher normalized counts in the western two quadrants (180°-360°, Figures 5.39c and 5.39d) at higher CTH's particularly at/above 2 km in the range between -20 and 0 dBZ. The northern two quadrants (270°-90°, Figures 5.39a and 5.39d) also have slightly lower ranges of the highest normalized counts (0.0005). -20 to 0 dBZ and -25 to -5 dBZ for the northeastern
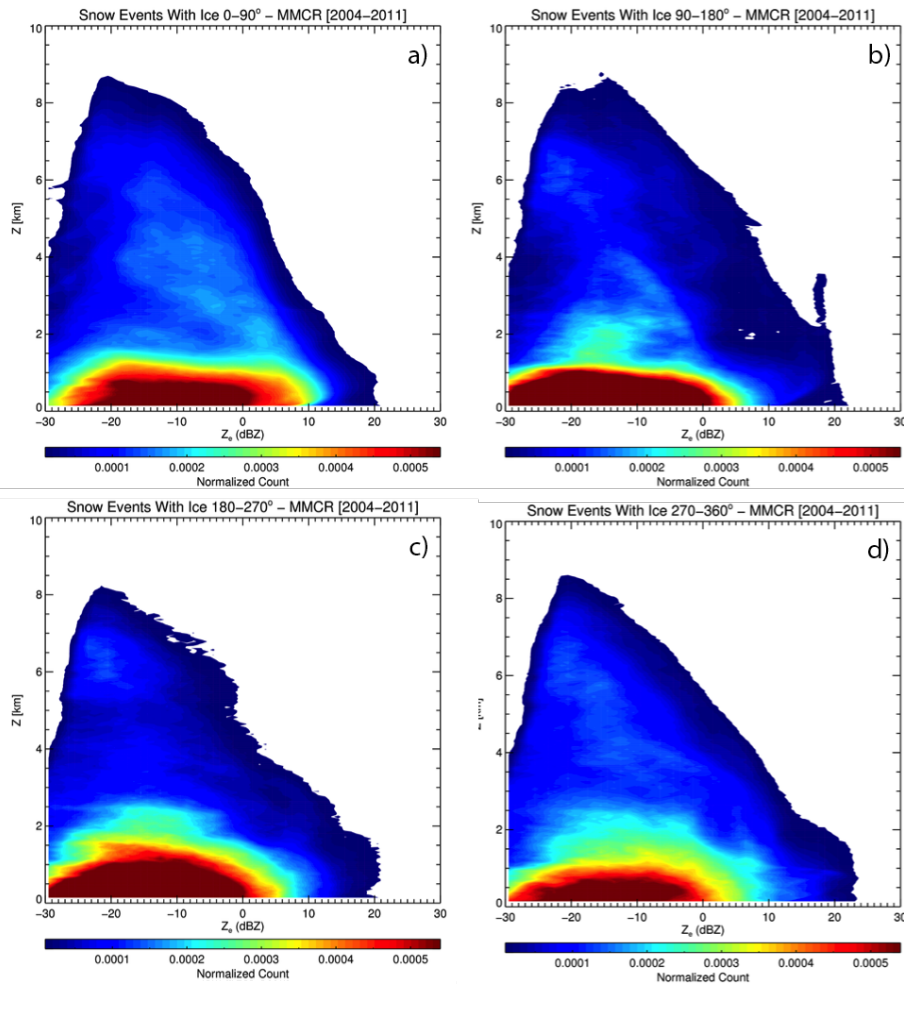
FIGURE 5.39: CFAD's displaying normalized snowfall observations for ice covered cases for each wind direction of 0°-90° (a), 90°-180° (b), 180°-270° (c), and 270°-360° (d), for the entire dataset

and northwestern directions respectively as compared to the two southern directions that have a range of -30 to 0 dBZ for the highest normalized counts.

The distribution of normalized counts is much different for open ocean cases, described in Figure 5.40. The majority of normalized counts are once again in shallow and low reflectivity regions, but the CTH's are shallower than ice covered cases, as most counts are below 1 km. The western two quadrants (Figures 5.40c and 5.40d) do show higher normalized counts at higher CTH's (0.0002+) above 1-2 km, for a similar range of reflectivity (-20 to 5 dBZ). The eastern two quadrants (Figures 5.40a and 5.40b) also have a smaller region of the highest normalized counts in comparison to the western two quadrants.
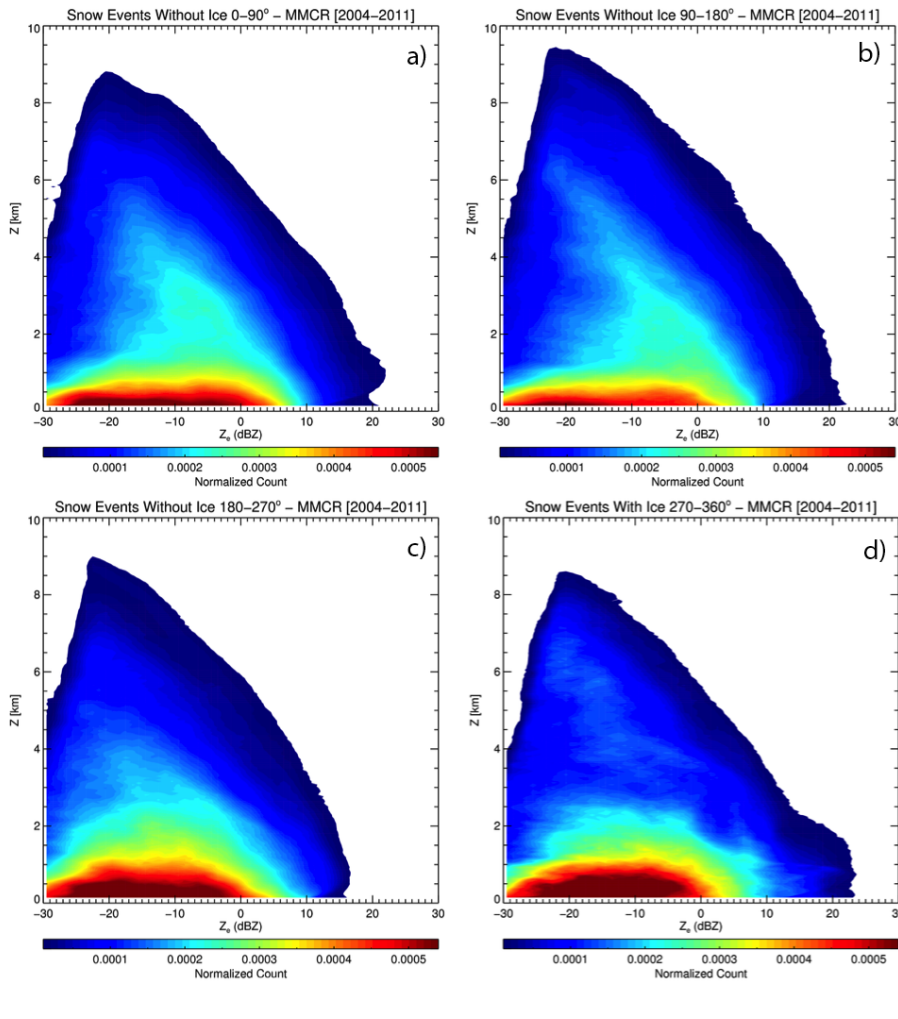
FIGURE 5.40: Same as Figure 5.39, but for open ocean events

Overall, the two cases show varying trends between each other. Ice covered cases show a very large region of the highest normalized counts in a shallow and light reflectivity area. The region with the highest normalized counts is in a similar area for open ocean cases, but the region is much smaller in comparison. There also tends to be higher normalized counts at higher CTH's for open ocean cases when compared to ice covered cases.

Snowfall rate is the final environmental parameter of interest as shown in Figure 5.41. Different processes for precipitation may occur for ice and no ice situations, thus using snowfall rate can be used to observe the difference in relative intensity. For larger snowfall rates (> 0.1 mmh^{-1}), the two cases are mostly the same, other than the small peak in relative frequency at 0.1 mmh^{-1} for open ocean cases. When snowfall gets lower, between 0.01 and 0.1 mmh^{-1},
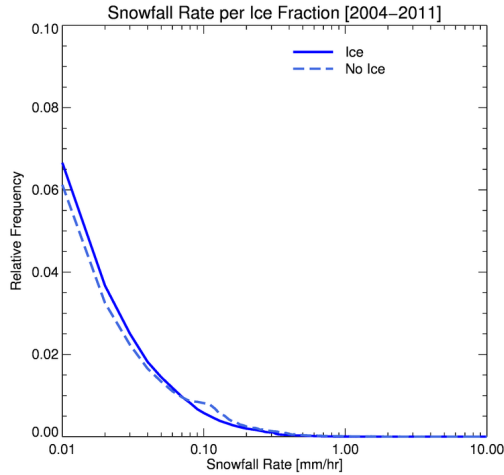
FIGURE 5.41: Relative frequency of occurrence of reflectivity for snowfall rate [mmh^{-1}] for ice covered and open ocean cases for the entire dataset
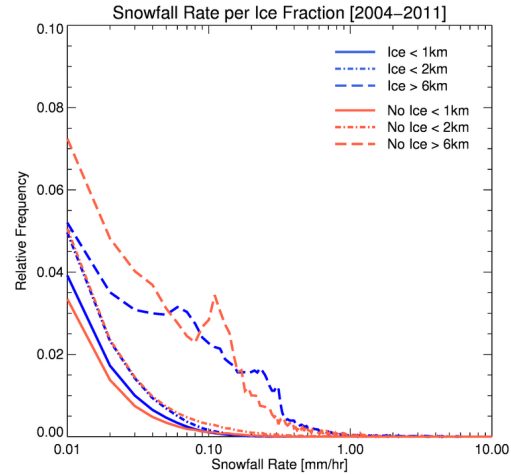
FIGURE 5.42: Relative frequency of occurrence of reflectivity for snowfall rate [mmh^{-1}] for multiple thresholds of cloud top height [km] for ice covered and open ocean cases for the entire dataset

the relative frequency of occurrence is slightly lower for cases with an open ocean than cases with an ice-covered ocean. Overall, not much separates the two cases in terms of snowfall rates.

When taking the same data and applying CTH thresholds, as shown in Figure 5.42, new information can be gathered about snowfall rates for each case. The individual thresholds show relatively similar characteristics for each case, however slight differences exist. For the lowest threshold where CTH's are less than 1 km, the two cases sharply decrease in relative frequency at the edge threshold of 0.01 mmh^{-1} until just above 0.1 mmh^{-1}. Cases with an ice covered ocean show higher relative frequency values throughout, despite roughly the same negative slope. Moving up a level to cases with CTH's below 2 km, the two cases are nearly the same until higher snowfall rates where open ocean cases have a very slightly higher relative frequency of occurrence. The last threshold involves deep snowfall observations of above 6 km and shows the most variability between the two cases. Starting at 0.01 mmh^{-1} the relative frequency of occurrence values are 0.07 and 0.05 for open ocean and ice covered cases respectively. Overall, these values decrease with increased

snowfall rate other than a few secondary peaks where the two cases once again differentiate themselves. Ice covered cases were below or even open ocean cases in terms of relative frequency except at just under 0.10 mmh^{-1} and for a small range between 0.1 and 1.0 mmh^{-1}. At just above 0.1 mmh^{-1}, there is a secondary peak for open ocean cases and is one of the only points above 0.1 mmh^{-1} where there is a higher relative frequency of occurrence. Overall, there isn't much to differentiate the two cases until the highest CTH threshold where variances exist.

5.5 Investigation of Ice Coverage Impacts – Section Summary

- The relative frequency of occurrence at higher/lower reflectivities is higher for open ocean/ice covered cases.

- No observable trend is consistent throughout all cloud layers as some thresholds have open ocean cases with higher relative frequency values at higher reflectivities (1 km < 2km, 2 km < 6 km) and others have ice covered cases with the same results (< 1 km, > 6km).

- The large grouping of temperature and relative humidity counts at temperatures above -10°C not associated with the positive trend, shown in Figure 33, is associated with open ocean snowfall events.

- For each case, wind direction shows relatively the same trend throughout, with small variability toward lower reflectivities, which is consistent at lower cloud level thresholds as well.

- Snowfall rates are relatively the same for each case and remain consistent with varying cloud level thresholds. The greatest variability occurs at higher cloud levels, where snowfall rates are prominently increased.

Chapter 6

Conclusions

Completing a study using a ground based radar to verify CloudSat data in an effort to improve future spaceborne radar platforms and advance the current knowledge of snowfall in Barrow, AK is beneficial for snowfall observations on both regional and global scales. Utilizing the seven year dataset at the NSA site and all that it provides allows for a complete overview of what is necessary to perform an effective study. Multiple steps were enacted to accomplish the primary goals of this research. The first of which included analyzing daily reflectivity profiles to gain a perspective for the various cloud regimes that persist in Barrow, AK. For the most part, the combination of shallow cloud top heights and light precipitation are predominant snowfall regime. This was verified when observing all counts of snowfall observations for the entire dataset and yearly dataset. On both a daily and yearly scale there was variability in terms of cloud top height and reflectivity, however as stated, observations with shallow cloud top heights and light reflectivity far exceeded those with deep or tall cloud top heights and high reflectivities. Specifically, two years from 2005-2007, where almost exclusively dominated by this snowfall regime and is worth further analysis in future research project.

The next step included taking those snowfall observations and gathering statistics in order to describe what is being missed in the near-surface spaceborne radar blindzone and convey the effectiveness of current and potential future spaceborne radar platforms. These statistics further confirmed the predominance in shallow and light snowfall. They also showed that about 10% of all snowfall CloudSat would deem 'snow certain' (greater than -7 dBZ) would

likely be missed in the blindzone and that about a third of all snowfall observations fall below one kilometer, directly in the blindzone. About 1/3 of all snowfall observations at Barrow, AK over the seven-year period of the dataset utilized for this dataset were below 1km. Snowfall observations above -15 dBZ, which is an endorsed threshold for snowfall, showed that about 18% of all snowfall observations that met this reflectivity threshold also fell below 1 km. When comparing the minimum detectable reflectivity of both GPM and the planned future ACE mission, a large amount of snowfall observations are overlooked, which is 85% and 67% respectively for all observed reflectivity. One way to potentially avoid the blindzone issue is by estimating reflectivity below the one kilometer AGL. In order to investigate this, vertical reflectivity correlations between the MMCR near surface bin (140 m AGL) and radar bins in the lowest two kilometers were taken for multiple cloud top height thresholds in order to observe how well reflectivity values at the surface correlate with reflectivity values at levels above it. This is valuable information because it tells whether or not reasonable estimations for surface reflectivity can be made for various snowfall regimes. The results were not promising for making estimations for shallow snowfall regimes, especially when compared to cases involving deeper snowfall regimes. Cases with deep snowfall events, cloud top heights greater than six kilometers, displayed very high correlations, about 0.8 at 1 km, meaning that estimations for surface reflectivity would likely be relatively accurate. However, cloud top height levels below two kilometers exhibited very low correlations, about 0.5 at 1km and near 0 at 1.5 km, promoting that making reflectivity estimations would likely be unreliable, thus, concluding that current and near future satellite observations likely underestimate the total amount of snowfall on a global scale.

The following step in this research was analyzing the multiple environmental parameters available through the NSA site in order to assess snowfall's dependencies on certain factors relating to each environmental parameter or a combination of parameters. Assessing wind speed and wind direction to identify where and what conditions persist for snowfall. Overall, the

majority snowfall observations occurred when the wind direction was from the northeast quadrant of a windrose. In general, there is no easily observable trend in terms of strength of snowfall event based on wind direction for the entire dataset, although, year to year, there are various trends, but they are not consistent. When observing temperature and relative humidity together to analyze what combination of those parameters led to the best conditions for snowfall, results show that there is a positive trend toward higher temperature and higher humidities and a large number of observations near higher temperatures.

Other results showed lower pressure corresponds to higher reflectivity and vice versa. This was consistent with the trends in cloud top height and reflectivity where as cloud top height increased, reflectivity increased. These results confirmed expectations where higher cloud top heights are generally associated with lower pressure system and thus would both produce higher reflectivities and vice versa for lower cloud top heights and higher pressure systems. Taking the same parameters and investigating their influence on snowfall rates show similar trends. Snowfall rates slightly increase with higher cloud top heights and lower pressure and vice versa for lower cloud top heights and higher pressure.

The last step in this research was to incorporate ice coverage analysis to further study snowfall regimes at Barrow, AK and how open ocean snowfall cases compare with ice covered snowfall cases. Results showed that each case was very similar in terms of relative strength using reflectivity, although some differentiation did exist when similar partitioning to earlier analysis was integrated. Cases with an open ocean showed higher relative frequency of occurrence values for higher reflectivities and vice versa for lower reflectivity values indicating open ocean cases were relatively stronger over the course of the dataset. When partitioned into cloud top height and pressure thresholds, the two cases were very similar and showed similar trends to earlier analysis, however at about 10 dBZ for open ocean cases, there was a large maximum in

relative frequency of occurrence for the deepest thresholds, highest cloud top height, lowest pressure. This is an interesting result as it is confirmed in two separate partitions.

Similar environmental parameter analysis can be done as well for each ice coverage case. For open ocean cases, temperatures were much higher than compared to cases where there was full ice coverage, which was expected. Utilizing wind direction data for each case also offered another perspective on what snowfall events depend on. For ice covered ocean cases, much like the earlier analysis, showed no clear trends for all directions, however open ocean cases showed some variability. The northern two quadrants were very similar to each other and all ice-covered cases, but the two southern cases were different as the south-western quadrant presented a higher relative frequency of occurrence value at 10 dBZ and the south-eastern quadrant decreased in relative frequency of occurrence as reflectivity increased, which is most likely due to the lack of any ocean effect from that direction.

Another way to analyze this parameter is to add a cloud top height threshold to investigate whether or not differences exist at multiple levels. For the shallowest case of less than one kilometer, both cases show similar trends where the relative frequency of occurrence decreases with higher reflectivities, but open ocean cases show slightly higher relative frequency of occurrence values at lower reflectivities and generally lower relative frequency of occurrence values at higher reflectivities. When moving up one kilometer to snowfall cases less than two kilometers, the results are different. A similar trend exists between most quadrants and cases, but there is no clear differentiation among each case like the results with the one-kilometer threshold. Also, the south-eastern quadrant with an open ocean stands out from the rest events as it doesn't follow the same trend and has a large maximum in relative frequency of occurrence at about 10 dBZ, so this case has stronger snowfall events during this period of study. The last parameter of interest was investigating snowfall rates in ice-covered and open ocean snowfall cases, which showed very similar

results overall indicating that the snowfall rates will be relatively the same no matter the ice coverage.

The final conclusions that result from this research are as follows for the satellite radar and snowfall community. Due to the undeniable amount of snowfall events that consist of cloud top heights below one kilometer, efforts to decrease the blindzone (1 km AGL) as much as possible should be taken. At minimum, acknowledgement of the underestimation of snowfall should be noted for any global snowfall retrieval. In general, the current minimum reflectivity of CloudSat (-30 dBZ) is set at an appropriate range, however this range is deemed nearly ineffective due to the blindzone. It is certainly a much more applicable range than GPM for measuring snowfall and should be considered the most suitable value for future spaceborne radar platforms. For snowfall, any minimum reflectivity above -15 dBZ still leaves a fair sized portion of potentially missed snowfall observations from an occurrence perspective, but the majority of accumulation occurrences are accounted for above this threshold. CloudSat is still an exceptional tool for measuring snowfall on a global scale, however, the results from this research should be noted and steps should be taken in order to improve future global snowfall retrievals.

Chapter 7

Future Work

One of the major assets of this type of research is the ability to easily expand the analysis to profiling radars at other sites. Barrow, AK isn't the only location that experiences very shallow and light precipitation on a regular basis, which means snowfall at other locations around the globe is also being underestimated by spaceborne radars due to its inherent blindzone that hinders true surface snowfall estimates. Expanding this type of research to other ARM sites (e.g., SGP) and other sites with profiling radars across the world would be very beneficial to the improvement of current global snowfall knowledge as well as provide more robust data for future spaceborne radar platforms to use.

Chapter 8

Bibliography

Cao, Qing et al. "Snowfall Detectability of NASA'S CloudSat: The First Cross-Investigation of Its 2C-Snow-Profile Product and National Multi-Sensor Mosaic QPE (NMQ) Snowfall Data." 148.April (2014): 55–61. Print.

Cassano, Elizabeth N et al."Classification of Synoptic Patterns in the Western Arctic Associated with Extreme Events at Barrow , Alaska , USA." 30.Wigley 1985 (2006): 83–97. Print.

Castellani, Benjamin B et al. "Journal of Geophysical Research: Atmospheres The Annual Cycle of Snowfall at Summit , Greenland." (2015): 6654–6668. Web.

Chen, Sheng et al. "Comparison of Snowfall Estimates from the NASA CloudSat Cloud Profiling Radar and NOAA/NSSL Multi-Radar Multi-Sensor System." Journal of Hydrology 541 (2016): 862–872. Web.

Curtis, J et al. "Precipitation Decrease In The Western Arctic, with Special Emphasis on Barrow and Barter Island, Alaska." 1707 (1998): 1687–1707. Print.

Hansen, Winslow D et al. "Changing Daily Wind Speeds on Alaska'S North Slope: Implications for Rural Hunting Opportunities Stuart Chapin, III and Gary P. Kofinas Source: Arctic , Vol . 66 , No . 4 (DECEMBER 2013), Pp . 448-458 Published by: Arctic Institute of North Ameri." 66.4 (2013): 448–458. Print.

Hiley, Michael, Mark Kulie, and Ralf Bennartz. "Uncertainty Analysis for CloudSat Snowfall Retrievals." (2011): 399–418. Web. Hinzman, Larry D et al. "Evidence and Implications of Recent Climate Change in Northern Alaska and Other Arctic Regions a Recent Synthesis of Evidence from Marine , Terrestrial and Atmospheric Stud- Ies Shows That the Climate of the Arctic Has Warmed Significantly in the Last 30 ." (2005): 251–298. Web.

Hou, Arthur Y. et al. "The Global Precipitation Measurement Mission." Bulletin of the American Meteorological Society 95.5 (2014): 701–722. Web.

Kulie, Mark, and Ralf Bennartz. "Utilizing Spaceborne Radars to Retrieve Dry Snowfall." (2009): 2564–2580. Web.

Kulie, Mark S. et al. "A Shallow Cumuliform Snowfall Census Using Spaceborne Radar." Journal of Hydrometeorology (2016): JHM-D-15-0123.1. Web.

Liu, Guosheng. "Deriving Snow Cloud Characteristics from CloudSat Observations." Journal of Geophysical Research Atmospheres 114.8 (2008): 1–13. Web.

Lynch, Amanda H, and Ronald D Brunner. "Context and Climate Change: An Integrated Assessment for Barrow , Alaska." (2007): 93–111. Web.

Maahn, Maximilian et al. "How Does the Spaceborne Radar Blind Zone affect Derived Surface Snowfall Statistics in Polar Regions?" May (2014): 604–620. Web.

Matrosov, Sergey Y., Matthew D. Shupe, and Irina V. Djalalova. "Snowfall Retrievals Using Millimeter-Wavelength Cloud Radars." (2007): 769–777. Web.

Moran, K P et al. "An Unattended Cloud Profiling Radar for Use in Climate Research" Bull. Am. Meteorol. Soc. 79 (1998): 443–455. Web.

Nolin, A, R Armstrong, and J Maslanik. "Near-Real-Time SSM/I-SSMIS EASE-Grid Daily Global Ice Concentration and Snow Extent. Version 4." Boulder, Colorado USA: NASA DAAC at the National Snow and Ice Data Center. N.p., 1998. Print.

Norin, L et al. "Intercomparison of Snowfall Estimates Derived from the CloudSat Cloud Profiling Radar and the Ground-Based Weather Radar Network over Sweden." (2015): 5009–5021. Web.

Shupe, Matthew D. et al. "A Focus on Mixed-Phase Clouds." Bulletin of the American Meteorological Society 89.10 (2008): 1549–1562. Web.

Stafford, J M, G Wendler, and J Curtis. "Temperature and Precipitation of Alaska: 50 Year Trend Analysis." 44 (2000): 33–44. Print.

Stone, Robert S et al. "Earlier Spring Snowmelt in Northern Alaska as an Indicator of Climate Change." 107 (2002): n. pag. Print.

Wang, Yonggang, Bart Geerts, and Yaosheng Chen. "Vertical Structure of Boundary Layer Convection during Cold-Air Outbreaks at Barrow, Alaska." Journal of Geophysical Research: Atmospheres (2015): 399–412. Web.

Wood, Norman B. et al. "Level 2C Snow Profile Process Description and Interface Control Document." D (2013): n. pag. Print.